This project has received funding from the European Union's Horizon 2020 research and innovation programme under grand agreement No 773715

Grant Agreement No.: 773715

Project acronym: RESOLVD

Project title: Renewable penetration levered by Efficient Low Voltage Distribution grids

Research and Innovation Action

Topic: LCE-01-2016-2017

Next generation innovative technologies enabling smart grids, storage and energy system integration with increasing share of renewables: distribution network

Starting date of project: 1st of October 2017

Duration: 36 months

D2.1 – Power electronics device design specifications and models for the architectures

Organization name of lead contractor for this deliverable: UPC	
Due date:	31th of March 2018
Submission Date:	28th of March 2018
Primary Authors	Francisco Díaz-González, Daniel Heredero-Peris, Andreas Sumper, Francesc Girbau-Llistuella, Mònica Aragüés; Stefan Marksteiner; Luisa Candido, Ramon Gallart-Fernandez
Contributors	UPC, JR, EYPESA
Version	Version 1.0

Dissemination Level		
PU	Public	X
CO	Confidential, only for members of the consortium (including the Commission Services)	

This project has received funding from the European Union's Horizon 2020 research and innovation programme under grand agreement No 773715

Deliverable reviews

Revision table for this deliverable:		
Version 1.0	Reception Date	01st of March 2018
	Revision Date	21st of March 2018
	Reviewers	Ramon Gallart Fernandez (EYPESA) Stefan Marksteiner (JR)

Table of contents

List of acronyms

BMS	Battery Management System
EMC	Electromagnetic Compatibility
ER	Energy Router
FTI	Fault Tolerance Index
ILEM	Intelligent Local Energy Manager
MMCC	Modular Multilevel Cascaded Converter
MTBF	Mean-Time Between Failures
PCS	Power Conversion System
PLC	Power Line Communications
PMU	Phasor Measurement Unit
SPWM	Sinusoidal Pulse Width Modulation
SSH	Secure Shell
TCP/IP	Transmission Control Protocol / Internet Protocol
TLS	Transport Layer Security
UPWM	Unipolar Pulse Width Modulation
VLAN	Virtual Local Area Network
VPN	Virtual Private Network
WAMS	Wide Area Monitoring System

Executive Summary

Energy storage systems are progressively gaining momentum in diverse strategic fields such as electromobility, renewable-based generation systems and power networks. In this regard, special emphasis is in electrochemical technologies, i.e. batteries. An energy storage system is composed by two main parts: i) a so-called power plane; and ii) a management plane. The power plane includes the components actually exchanging electrical power with the network; this system is connected to, e.g. batteries and power electronics. In turn, the management plane is composed by algorithms and related hardware managing the aforementioned system. A kind of structure is adopted for the power electronics device with local storage, the Energy Router (ER) hereinafter, to be developed in the RESOLVD project.

The design of both the power and management planes of the ER can be diverse and it greatly determines the capability and performance of the system. Accordingly, the objectives of the present work are:

- The selection of the architecture of the power plane of the ER, i.e. of the way the different power electronics-based modules are interconnected between them, thus building up a modular design and providing the ER with maximum flexibility, efficiency, fault tolerance, reliability and minimum volume.
- The statement of the practical aspects related to electrical engineering to take into account while actually integrating the ER, as a new equipment, into low voltage grids. These aspects refer, for instance, to conduced and radiated electromagnetic compatibility with other devices and the easy installation in grids.
- The statement of the aspects to take into account in regard of the security implications of the interaction of the algorithms included in the management plane of the ER interfacing with the rest of the RESOLVD grid management tools (i.e. cybersecurity assessment).

So the present work mainly tackles the power plane of the ER, leaving a deep study on the management plane to other tasks of the RESOLVD project.

Addressing the main objectives of the project, the contents of the present work are structured as follows. Section 2 describes the general architecture of the ER, differentiating among the power plane and the management plane of the invention. Then, section 3 addresses the power plane of the ER by comparing diverse architectures based on an extensive literature review and state-of-the-art computational methods. From the work in this section, the best way to interconnect the power converters comprising the ER can be concluded. Once the architecture for the power plane of the ER has been addressed, section 4 presents two further important aspects to take into account at the time of designing the ER, and these has to do with the interaction of the ER with other network components. Firstly, section 4.1 addresses practical aspects related to the commissioning and operation of the ER in low voltage networks. Secondly, section 4.2 tangentially attends the management plane of the ER by listing aspects to take into account while designing the algorithms and communication capabilities of the device in regard of cybersecurity. After all above mentioned sections, the report summarizes the principal conclusions in section 5. The last principal point of the report is the inclusion of an annex briefly describing the modelling of the power converters building up the power plane of the ER. These models are to be exploited in subsequent tasks of RESOLVD project.

Power plane architecture

One of the straightforward strategies to connect a modular battery-based system to the grid is configuring a Power Conversion System (PCS) based on the idea of parallelizing inverters, each one holding part of the total number of battery cells in series/parallel configuration. For the purposes of the present work, this would result in a PCS called *number #1*, which can be deployed in the variants #1a through #1c. The variant #1a, proposes the direct connection of a certain number of battery cells in the dc-link of the inverter of a module, or power train. In

contrast, #1b interfaces a dc-dc conversion step between the battery cells and the dc-link of the inverter. Further, the PCS number #1c provides this dc-dc conversion step with galvanic isolation. See the graphical explanation in Figure A. This definition of variants, or different topologies at module level, is also adopted for the presentation of all PCSs in this work.

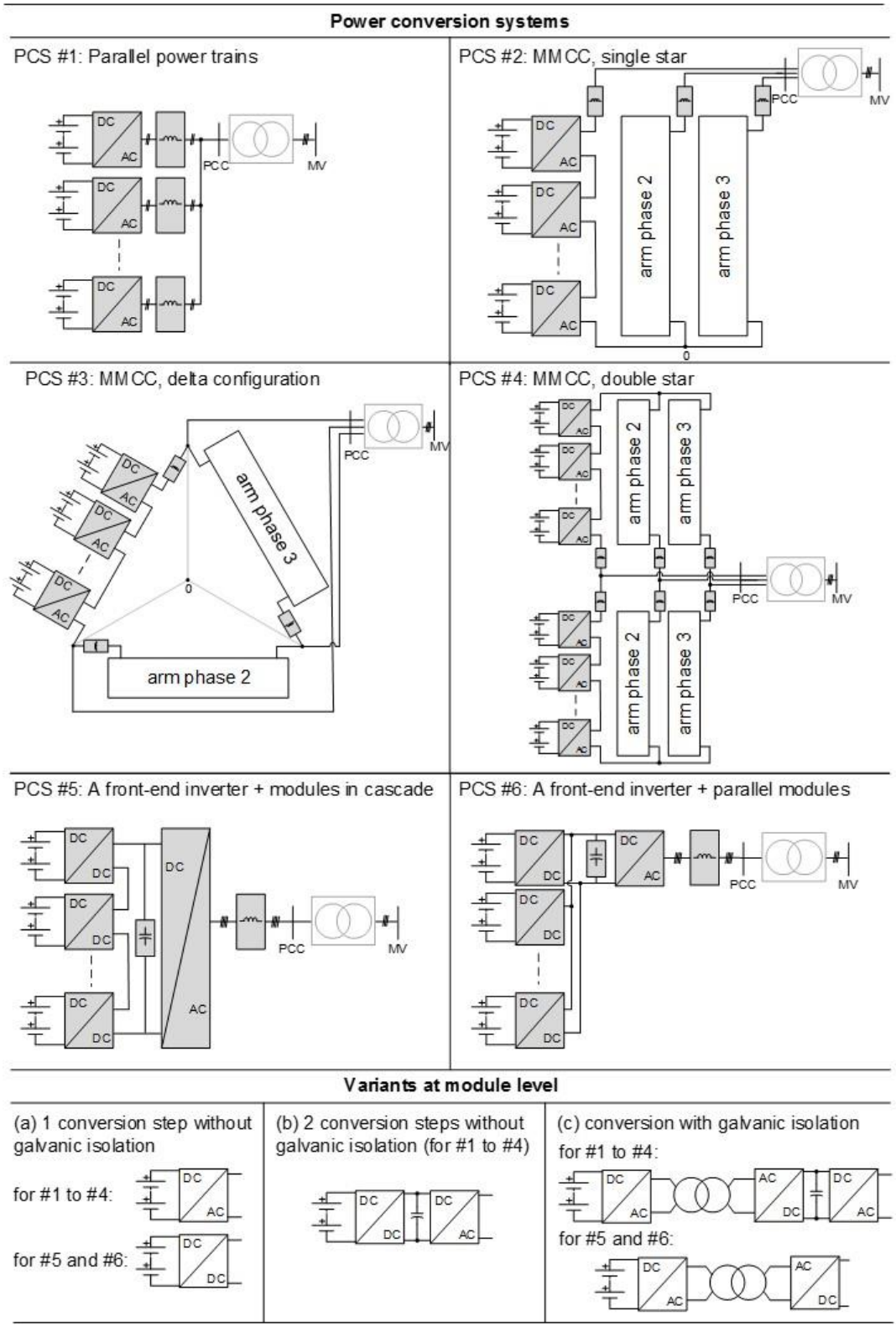

Figure A: Power conversion systems (PCSs) for modular battery-based energy storage systems.

To compare all six PCS architectures previously presented in a fair way, some assumptions are adopted. The comparisons focus on various aspects such as reliability, efficiency, fault handling, compactness and flexibility. These aspects are addressed since they are being considered as principal for the design of PCSs. The latter aspect refers to the possibility of effectively configuring hybrid energy storage solutions by including different types of batteries. Some of the most important assumptions are listed in the following:

- The solution, as a whole, is rated at 30 kW and 60 kWh regardless the PCS topology. These power and energy storage capacities are distributed in 6 modules. Each module is composed by a battery pack and associated power conversion system rated at 5 kW / 10 kWh.
- The phase-to-phase voltage at the low voltage side of the coupling transformer of the PCSs with the external network is 400 V (phase-to-phase) for all cases.
- The rated voltage of each of the 6 battery packs configuring the system is 400 V.
- The switching schemes for the different dc-dc and dc-ac converters building up the different PCSs are adopted from the state-of-the-art in this matter.
- Given the voltage at the battery pack terminals, the voltage and the connection point of the PCS and the switching schemes, the voltages at the terminals of each of the modules composing the different PCSs are selected as the minimum recommended for a proper operation of the power electronics.
- The transistor modules for each of the dc-dc and ac-dc converters of the different PCSs are differentiated with respect to the electrical magnitudes they should withstand.

Based on the different exercises comparing PCSs, following contents remark the most important aspects:

- PCS #1 through its different variants is identified as the most convenient option addressing all criteria considered in this work. It is reliable, efficient, flexible, compact, and offers good performance under faults.
- PCS #6 follows PCS #1 in most of the criteria considered in this work. Thus, it is considered also as a good candidate for modular battery based solutions, with the potential of even improve the performance of PCS #1, by using less power converters.
- MMCC structures, as those considered in PCS #2 through #4, are identified as promising options in the future. Research and development should concentrate here in the development of power sharing algorithms that ensure the balance of charge among the different battery packs. This would permit to overcome the drawbacks of connecting in cascade different battery packs.
- Finally, PCS #5 is identified as the weakest configuration among the eligible. The connection of different battery packs in cascade, configuring a medium voltage dc-link that is to be managed by a single three-phase front-end inverter, is identified as a hardly reliable option, as well as poorly flexible and efficient one.
- As the principal outcome of the above exercise, the PCS #6 variant c) was determined as the most convenient one for the purposes of the present work. However PCS #1 is identified a slightly superior solution than PCS #6 currently, it is worth to investigate within RESOLVD project in PCS #6 as it has the potentiality to become a solution with similar performance of PCS #1 employing a less number of power converters. PCS #6 variant c) offers an excellent reliability, efficiency, compactness and behavior under grid faults. In addition, it offers excellent flexibility while integrating different batteries of different characteristics, thus addressing one of the main requirements for RESOLVD project.

Complementing such conclusions, Figure C offers a graphical comparison among PCSs.

Assessment on the interaction with network devices: practical aspects for grid integration and cybersecurity

Complementing the decision on the architecture of the power plane of the Energy Router, important aspects regarding the electrical integration of the device into networks have been identified. Such exercise results into a relevant list of issues that should be addressed at the time of actually designing the prototype of the ER in subsequent tasks of the project (e.g. the assessment of EMC noise, the easy installation of the device in grids and the operation of the ER under failures in communication systems, among others).

Finally, section 4.2 offers a first assessment on cybersecurity aspects that should be taken into account at the time of designing the management plane of the ER. Work included a threat model, through which a list of 41 potential threats for the ER while interfacing with other network devices was presented. After this first exercise, a first discussion on cybersecurity measures was presented. Several aspects were addressed, including the physical device security, the network access security, the logging and monitoring considerations, communication line security issues and data storage security.

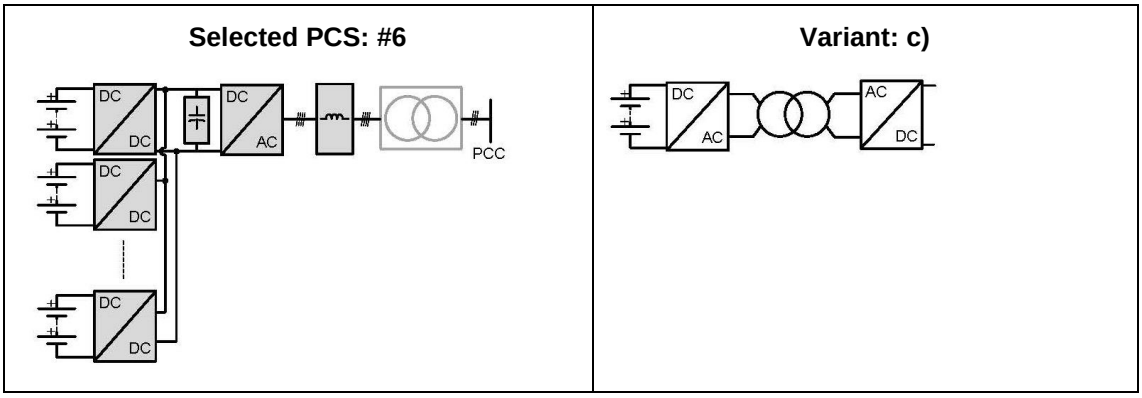

Figure B: Selected PCSs for modular battery-based energy storage systems.

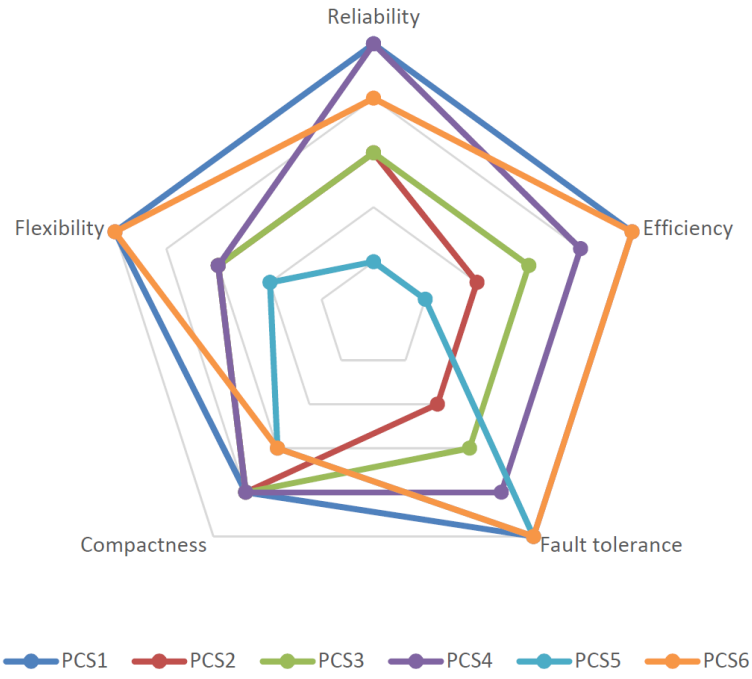

Figure C: Comparison synthesis among PCSs.

1. Introduction

1.1. Objectives

Energy storage systems are progressively gaining momentum in diverse strategic fields such as electromobility, distributed renewable-based generation systems and power networks. In this regard, special emphasis is in electrochemical technologies, i.e. batteries. One indicator of this is the fact that at the time of writing this article, 60% of about the 1650 projects listed in [18] are around electrochemical technologies - an institutional database (Department of Energy of the United States) collecting projects involving the implementation of energy storage systems in different environments related to electric vehicles, renewables and power networks worldwide.

An energy storage system is composed by two main parts: i) a so-called power plane; and ii) a management plane. The power plane includes the components actually exchanging electrical power with the network; this system is connected to, e.g. batteries and power electronics. In turn, the management plane is composed by those algorithms and related hardware managing the aforementioned system. A kind of structure is adopted for the power electronics device with local storage, the Energy Router (ER) hereinafter, to be developed in RESOLVD project.

The design of both the power and management planes of the ER can be diverse and it greatly determines the capability and performance of the system. Accordingly, the objectives of the present work are:

- The selection of the architecture of the power plane of the ER, i.e. of the way the different power electronics-based modules are interconnected between them, thus building up a modular design and providing the ER with maximum flexibility, efficiency, fault tolerance, reliability and minimum volume.
- The statement of the practical aspects related to electrical engineering to take into account while actually integrating the ER, as a new equipment, into low voltage grids. These aspects refer, for instance, to electromagnetic compatibility with other devices and the easy installation in grids.
- The statement of the aspects to take into account in regard of the interaction of the algorithms included in the management plane of the ER interfacing with the rest of the RESOLVD grid management tools (i.e. cybersecurity assessment).

So the present work mainly tackles the power plane of the ER, leaving a deep study on the management plane to other tasks of RESOLVD project.

In regard of the power plane, three main subsystems are differentiated: i) the energy storage containers, e.g. the batteries; ii) the power conversion system, e.g. the power electronics; and iii) ancillary balance of plant components, e.g. cooling, protections, monitoring subsystems and etcetera. Power conversion system (PCS) is as important as the storage container itself, since it permits a controlled, secure and efficient power exchange with the system the energy storage system is connected to. The topology of PCSs can be diverse depending on many factors, such as the size of the energy storage system, as well as on the requirements on efficiency, reliability, volume, modularity and so on. Precisely while facing a modular energy storage system, the industry and the academia have proposed so far diverse proposals and their study and comparison is, as introduced before, one of the main objects of the present work.

Recent literature addressed a comparison of different PCSs for energy storage systems [5], [10], [13], [81], [99]. Research in [13] and [10] propose a general qualitative comparison among different PCSs. These can be intended as a general high level approach to the knowledge field. On higher level of detail, for instance in [5], a quantitative comparison among different structures based on Modular Multilevel Cascaded Converter (MMCC) are addressed. The comparison concentrates on efficiency and the dynamic performance. Similarly, [99] addressed a comparison between two types of PCSs: i) one composed by the grid connection through a three-phase inverter of a set of battery packs assembled in series and parallel configuration; ii) an MMCC-based converter with distributed battery backs in its modules. This work offers an

excellent quantitative comparison addressing fault tolerance, modularity and reliability of both PCSs. In [81], emphasis is also on the above related PCSs by [99]. Complementing the latter work, [81] address the efficiency aspect.

Complementing the literature described above, the present work proposes a qualitative and quantitative comparison among different PCSs for modular energy storage systems. The present work contributes in covering at once the most widely proposed PCSs, according to a literature review. Further, the present work addresses several aspects in regard of the comparison among PCSs, such as: reliability, efficiency, fault tolerance, compactness and flexibility. The latter aspect, among others, refers to the possibility of hybridizing the storage solution by including batteries of different characteristics. Altogether, the exercise carried out in this work, aims to provide general criteria at the time of designing a modular battery-based solution. The assessment of the different comparison criteria is based on state-of-the-art techniques, and with the aim of comparing the different PCSs in a fair way, common assumptions for all PCSs are adopted. Such comparison permits to come up with the best architecture for the PCS among eligible. This exercise is complemented with the description of simulation models for the selected PCS architecture that will be utilized in subsequent tasks of RESOLVD project.

The previously described contents, along with the statement of practical aspects for the grid integration of the device, both addressing electrical engineering and cybersecurity, complete the contents included in the present work.

1.2. Contributions of partners

Partner	Contribution
UPC	Leading contributor. Author of sections 1, 2, 3, 5 and annexes.
EYPESA	Contributor on practical aspects for the DSO grid integration of the power electronics device into electrical networks. Author of section 4.1.
JR	Contributor on cybersecurity aspects. Author of section 4.2.

1.3. Report structure

Addressing the main objectives of the project, the contents of the present work are structured as follows. Section 2 describes the general architecture of the ER, differentiating among the power plane and the management plane of the invention. Then, section 3 addresses the power plane of the ER by comparing diverse architectures based on an extensive literature review and state-of-the-art computational methods. From the work in this section, the best way to interconnect the power converters comprising the ER can be concluded. Once the architecture for the power plane of the ER has been addressed, section 4 presents two further important aspects to take into account at the time of designing the ER, and these has to do with the interaction of the ER with other network components. Firstly, section 4.1 addresses practical aspects related to the commissioning and operation of the ER in low voltage networks. Aspects such as electromagnetic compatibility, grounding and behaviour under electrical grid faults are to be included here. These aspects are principal for a successful design and integration of the ER into grids. Secondly, section 4.2 tangentially attends the management plane of the ER by listing aspects to take into account while designing the algorithms and communication capabilities of the device in regard of cybersecurity. After all above mentioned sections, the report summarizes the principal conclusions in section 5. The last principal point of the report is the inclusion of an annex briefly describing the modelling of the power converters building up the power plane of the ER. These models are to be exploited in subsequent tasks of RESOLVD project.

2. General architecture of the power electronics device (the Energy Router)

The Energy Router is a power electronics-based device equipped with local energy storage providing flexibility to low voltage grids. As an energy storage system, it can enhance the operation and power quality of low voltage grids by, for instance, contributing to the security of supply for costumers in case of grid eventualities; exchanging active and reactive power flows with the network following economic and / or technical criteria; and compensating current harmonics through cables affecting customers.

The Energy Router is composed by two main subsystems, which are framed into a power plane and into a management plane. The components included within the power plane are those actually exchanging power with the external network the ER is connected to. So in this regard, we find here batteries and the power electronics. The power plane of the ER is modular, so this means that it concerns different batteries of different characteristics connected to diverse power electronics modules. These modules are smartly interconnected providing best efficiency, flexibility, reliability and fault tolerance to the ER, and this is one of the key features of the invention.

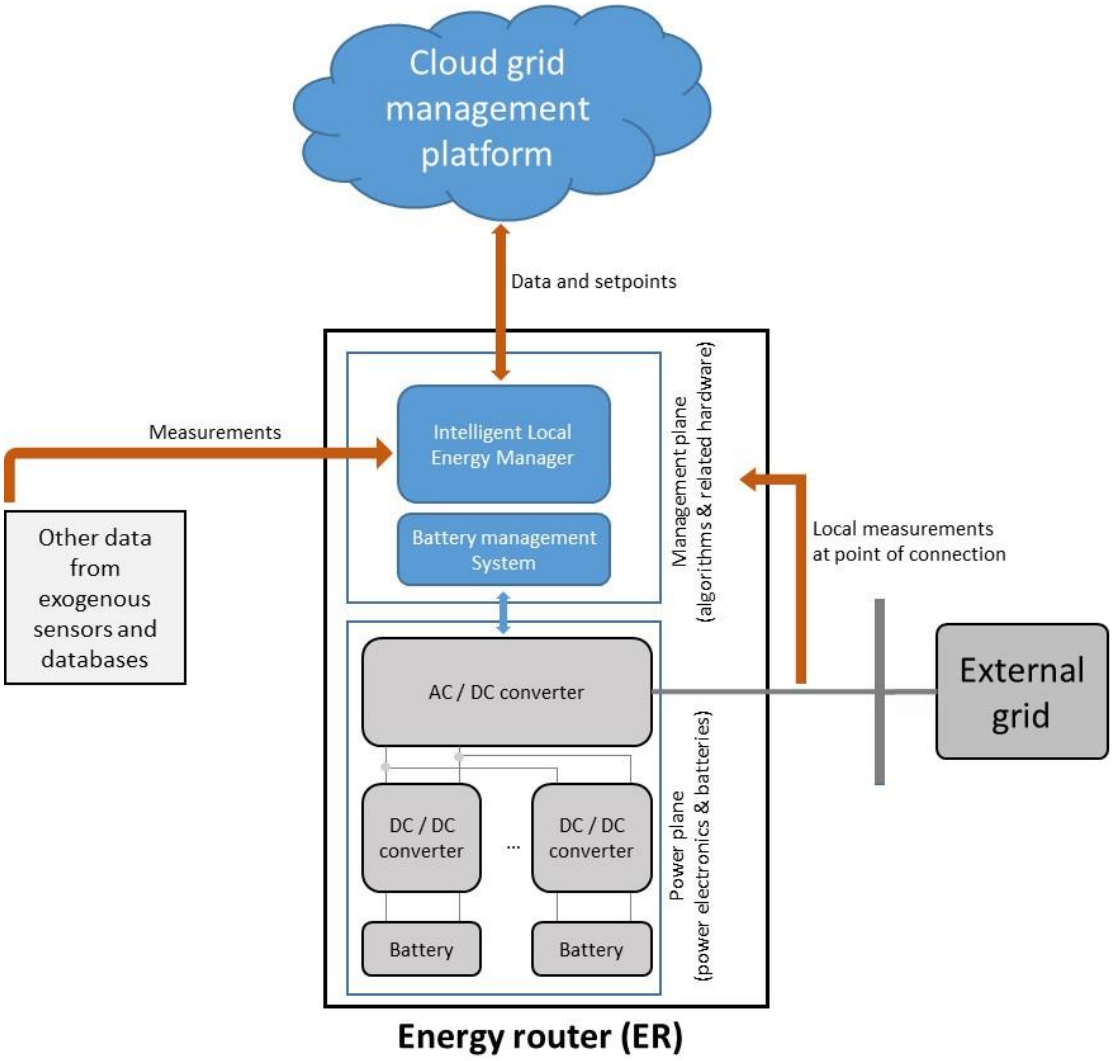

Figure 1: General architecture of the Energy Router.

Within the management plane mentioned above, we find the algorithms managing the operation of the ER, as well as the hardware (communication devices, processors, and etcetera) that either run algorithms or enable the exchange information with the exterior. The management architecture of the ER concerns, in turn, diverse layers, and it interacts with the management tools of the whole network. Figure Z plots a general architecture for the ER. As can be noted, the management plane is composed by a front-end algorithm which is called Intelligent Local Energy Manager (ILEM hereinafter). This algorithm receives (through the corresponding ICT tools spread through the network and those embedded into the ER), exogenous information and setpoints. From these, the ILEM controls the power exchange of the ER with the network. It can also decide whether or not follow exogenous setpoints in case of eventualities. The scope of the ILEM and the way it interacts with the rest of the network is to be fully addressed in other tasks of RESOLVD project.

Anyhow, given a power setpoint from the network operator, the ILEM would receive it and if convenient, transmit it to a second algorithm which is called Battery Management System (BMS). The BMS then performs different actuations directly interacting with batteries and DC/DC converters. In regard of the interaction with ILEM, it would translate the above mentioned power setpoint to diverse setpoints to the batteries connected to the ER. The setpoints such batteries receive, are adapted to the capacities, performance and availability of each one. In this regard, the BMS enables an optimal utilization of the energy storages embedded into the ER. The above described function is addressed hereinafter as a power sharing strategy among batteries. Other functions performed by the BMS have to do with the supervision of the state of charge and state of health of batteries. Such information is needed for proper power sharing among batteries.

3. Comparison of power conversion systems for modular battery-based energy storage systems

This section addresses one of the main objectives of the work, which is to compare different PCS architectures for the modular battery-based energy storage system. To do so, following contents are distributed into three main subsections. Firstly, subsection 3.1 summarizes the six main architectures to be considered, based on an extensive literature review. Secondly, subsection 3.2 develops diverse qualitative and quantitative analyses comparing architectures. Finally, subsection 3.3 synthetizes the main conclusions achieved from the previous exercises.

3.1. Classification of power conversion systems

One of the straightforward strategies to connect a modular battery-based system to the grid is configuring a PCS based on the idea of parallelizing inverters, each one holding part of the total number of battery cells in series/parallel configuration. For the purposes of the present work, this would result in a PCS called number #1, which can be deployed in the variants #1a through #1c. The variant #1a, proposes the direct connection of a certain number of battery cells in the dc-link of the inverter of a module, or power train. In contrast, #1b interfaces a dc-dc conversion step between the battery cells and the dc-link of the inverter. Further, the PCS number #1c provides this dc-dc conversion step with galvanic isolation. See the graphical explanation in Figure 2. This definition of variants, or different topologies at module level, is also adopted for the presentation of all PCSs in this work.

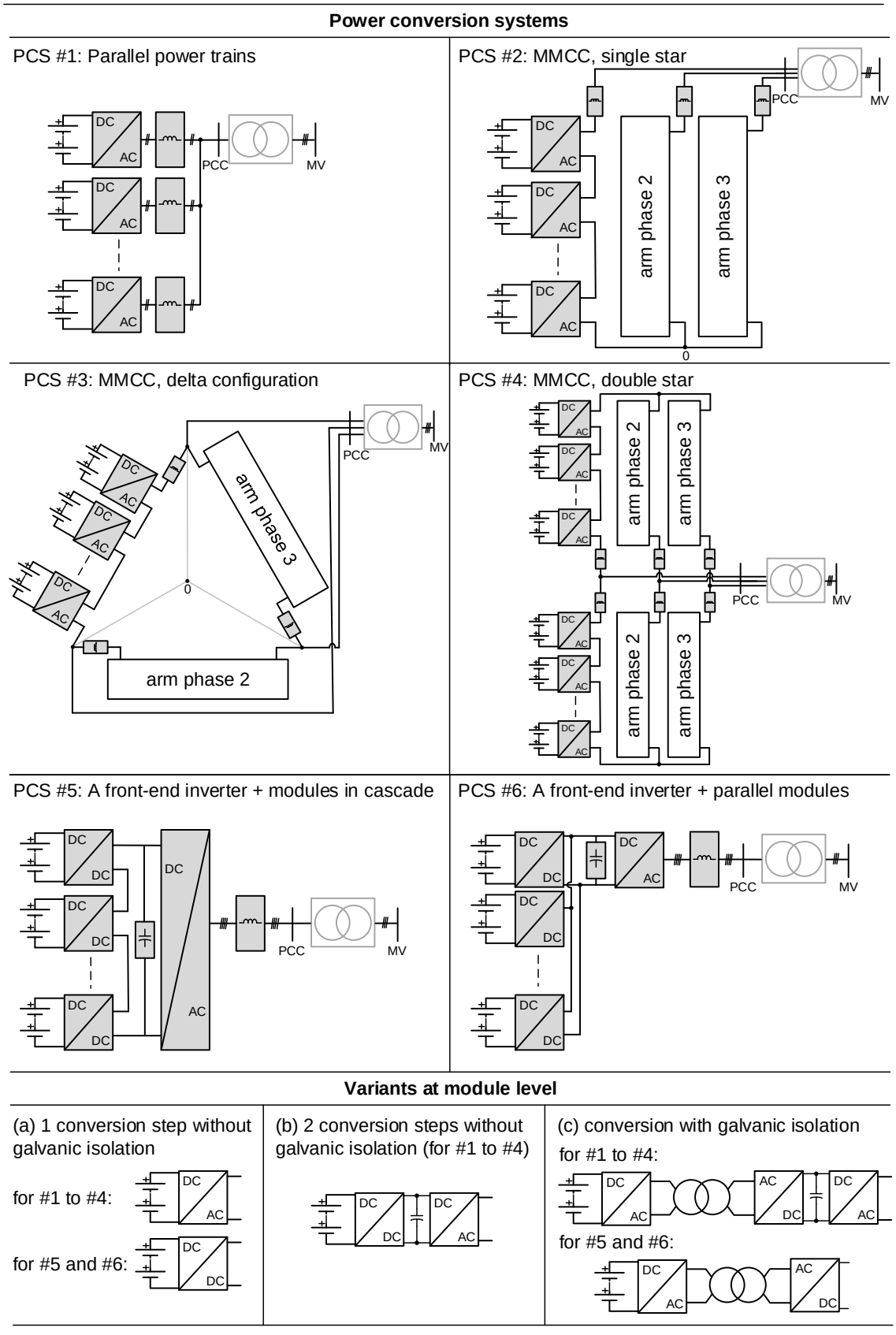

Figure 2: Power conversion systems (PCSs) for modular battery-based energy storage systems.

The above strategy is highly reliable, since the failure of one power inverter does not disable the whole storage system. Other proposals in between the adoption of a non-modular PCS and fully modular PCSs as proposals #1a through #1c, have been already defined in literature. Contributing to the catalog of PCSs for storage systems started above, the PCSs number #2 through #4 are based on the adoption of modular multilevel cascaded converters (MMCCs). The PCS number #2 corresponds to a MMCC, in which the modules are connected in cascade so that they configure three arms. These arms share one common point configuring a single star. The topology for each of the modules may perform a single step dc/ac conversion without including galvanic isolation, yielding in this case the variant #2a. This one step conversion can be realized by an H-bridge cell (or bridge cell hereinafter), or through a half-bridge cell (or chopper cell hereinafter). Analogous to the definition of variant #1b, variant #2b concerns a two-step dc-ac conversion at module level, interfacing one dc/dc conversion phase. In turn, this dc-dc conversion phase, while provided with galvanic isolation, defines the variant #2c.

Similarly to what is suggested for PCS number #2, the structure of a PCS number #3 corresponds to a MMCC. However, the three arms of modules connected in cascade do not share any common point, but they are connected between them in delta configuration. Depending on the topology of each module, variants #3a through #3c are defined analogously to variants #1a through #1c (or #2a through #2c).

Going further, one can extend the ratings of the PCS number #2 by doubling the number of arms building up the converter, so proposing 6 arms. In this configuration (named PCS number #4) each 3 arms share one common point thus configuring two stars (see Figure 2). Analogously to previous PCSs, variants #4a through #4c propose different topologies at module level.

In the previously presented PCSs number #2 through #4, the ac terminals of a MMCC inverter are the front-end power electronic interfaces, from which the PCS can be coupled to an external grid (including a passive filter and/or galvanic isolation in between though). Conversely, the PCS number #5 relies also on a cascade association of H-bridge modules, but performs a dc/dc conversion instead of a dc/ac transformation. In this PCS number #5, the front-end dc terminals of the cascade association are connected to an inverter, which couples the system to the external grid. The dc/dc conversion step at each module of the cascade association can be provided with galvanic isolation or not, yielding variants #5c and #5a respectively. The variant #5b (2 power conversion steps at module level), does not apply for this PCS. Finally, while the modules in the PCS number #5 are connected in cascade, the PCS number #6, along with its variants #6a and #6c, propose conversely their parallel connection.

To conclude, it is important to note that for PCSs number #1, #5 and #6, the topology of the front-end inverter can be realized in the form of the well-known 2-level H-bridge structure, or as a multilevel neutral point clamped structure (NPC), being the 3-level NPC structure the most approachable one.

Figure 2 graphically resumes the whole catalog of proposed PCSs. As a general note, please note that shaded boxes depicting dc-ac and dc-dc terms simply indicate the inclusion of power conversion blocks or modules, regardless the intended number of conversion steps and power electronics topology. In the same manner, shaded boxes depicting capacitor and inductance symbols simply represent the location of passive components, regardless their type and design. Further, the light gray coloring the transformer included in each of the PCSs in Figure 2, indicates that the inclusion of this equipment at the point of common coupling with the external grid is optional. Alternatively, the provision of the required galvanic isolation to the battery cells can be shifted to the module level (as intended for PCS variant (c)).

Table 1 summarizes literature on the previously defined PCSs, covering both experiences in industry and academic research. Please note that literature works reporting field experiences are marked in bold, and patents are noted in italics. As it can be noted, the few field experiences reported in the table adopt the PCS number #1, aiming to configure a highly redundant and reliable structure based on proven voltage source inverter technology. Alternatively, most of the academic research concentrates on the advance in MMCC-based

structures. It is interesting to note also that the majority of cited literature concern one power conversion step modules. This way, the required galvanic isolation is in most of the cases shifted to the point of connection with the external network, as indicated in Figure 2.

	Variants at module level			Applications
	(a) 1 conv. step (w/o galvanic isolation)	(b) 2 conv. step (w/o galvanic isolation)	(c) conversion with galvanic isolation	
#1: parallel power trains	[95], [13]	[13], **[65], [80], [66],** *[33]*	[101], [83]	EV motor drives, power network.
#2: MMCC single star	[86], [87], [49], [50], [51], [35], [72], [100], [85], [37], [89], [6]	[60], [92], [88]	[93]	EV motor drives, power network.
#3: MMCC delta configuration	[2]	[88]	[92], [93]	Power network.
#4: MMCC double star	[81], [26], [90], [4], [21], [70], [68], *[16]*	[8]	[30]	EV motor drives, power network, HVDC.
#5: A front-end inverter + modules in cascade	[59], [45], [10], *[9]*, *[69]*	Does not apply	[62], [63], [64], *[34]*	Power network, EV charger.
#6: A front-end inverter + parallel modules	[46], [73], [11], [97], *[74]*	Does not apply		Power network, EV motor drives.

[1] This work proposes a 1-phase converter.

[2] Dc-dc conversion step is based on half-bridge modules, and not H-bridge ones.

[3] This work concentrates on the dc-dc conversion step. The additional front-end inverter, as expected for PCSs \#5, is not included since not required.

[4] This work does not concern the inclusion of batteries, but supercapacitors.

Table 1: Literature on PCSs for modular battery-based storage systems. Works reporting field experiences are marked in bold, and patents are noted in italics.

The PCSs considered in this work are identified as the most proliferated ones in literature. However, such a classification does not exclude the existence of other proposals. For the sake of completeness, some of them are listed in the following since considered particularly interesting:

- (Patent). A PCS composed by (from the connection point with the grid to battery packs) [41]: i) an ac-dc and dc-ac H-bridges in back-to-back configuration; ii) the parallel connection of high frequency transformers; iii) the inclusion of an ac-dc conversion step interfacing each of the transformer terminals and a battery pack.
- (Article). A PCS composed by (from the connection point with the 3-phase motor of an EV to battery packs) [79]: i) an ac-dc 3-phase inverter; ii) the cascade connection of dc-dc modules interfacing with different battery packs. The dc-dc modules include galvanic isolation, as for PCSs variant (c). So such description fits with PCS #5, however it is different in the sense that the cascade connection of dc-dc modules also includes a series capacitor and altogether yield the total voltage of the dc-link. The inclusion of such capacitor permits the dc-dc converters to exchange a power proportional to the difference between the total dc-link voltage and the batteries. At the end, this results into a smaller converter compared to PCS #5.

The following sections deepen the comparison among the various PCS topologies for modular battery-based solutions identified and classified in Figure 2.

3.2. Comparison among power conversion systems

The previous section provides a first picture on PCSs for modular battery-based energy storage solutions. Further elaborating in the concepts presented there, this section offers a comparison among different PCSs, focusing on various aspects such as reliability, efficiency, fault handling, compactness and flexibility. These aspects are addressed since they are being considered as principal for the design of PCSs. The latter aspect refers to the possibility of effectively configure hybrid energy storage solutions, by including different types of batteries. With the aim of conducting a fair comparison among PCSs, some assumptions are firstly stated, and these are presented in the following subsection.

3.2.1. Assumptions

The following assumptions are adopted:

- The solution, as a whole, is rated at 30 kW and 60 kWh regardless the PCS topology. These power and energy storage capacities are distributed in 6 modules. Each module is composed by a battery pack and associated power conversion system rated at 5 kW / 10 kWh.
- The phase-to-phase and neutral voltage at the low voltage side of the coupling transformer of the PCSs with the external network is 400 V (phase-to-phase) for all cases.
- The rated voltage of each of the 6 battery packs configuring the system is 400 V. Packs are configured by standard 18650 type Lithium-ion cells [91]. A figure of merit for the capacity of each cell is usually around 2.5 Ah and the rated voltage is $V_{cell} = 3.7$ V, so to achieve 400 V at the pack terminals, 108 cells should be connected in series. Considering now the capacity of each string (2.5 Ah), to reach the required energy capacity of 10 kWh for the pack, 10 strings should be connected in parallel. The internal resistance of a cell, r_s, is in the range of milliohms (e.g. 55 mOhm) and the voltage at end-of-charge condition (fully charged) is $V_{cell_{eoc}} = 4.2$ V.
- The switching schemes for the different dc-dc and dc-ac converters building up the different PCSs are adopted from the state-of-the-art in this matter. A summary of the basis for each of them is presented in subsection 3.2.1.1. Detailed explanations are offered latter in the section.
- Given the voltage at the battery pack terminals, the voltage and the connection point of the PCS and the switching schemes, the voltages at the terminals of each of the modules composing the different PCSs are selected as the minimum recommended for a proper operation of the power electronics. This favors the performance of the PCSs. Further details on the calculation of voltage levels are offered in subsection 3.2.1.2.
- The transistor modules for each of the dc-dc and ac-dc converters of the different PCSs are differentiated with respect to the electrical magnitudes they should withstand. For 5 kW converters, the selected module is the model PS-22A78-E from Mitsubishi [58]. For low voltage ac-dc inverters of 30 kW (i.e. the front-end inverter in PCS #6), the selected module is the model QID3310006 from Mitsubishi [58]. The latter is also the module selected for medium voltage ac-dc inverters (i.e. the front-end inverter in PCS #5). The selection of the modules above is important for power losses calculation.

3.2.1.1. Switching schemes

The switching principles for H-bridge ac-dc, dc-dc as well as for MMCC structures are detailed in the following.

H-bridge ac-dc converters

H-bridge ac-dc converters are all operated under the two level SPWM switching technique [27]. For one-phase H-bridge inverters, this is based on the application of two sinusoidal carrier signals, one per each of the arms of the converter, which are shifted π rad between each other. These two carriers are compared to a triangular high-frequency signal, and from these comparisons, the duty cycle for each of the two branches are deduced. Such operating mode permits to obtain, at the mid point of each branch and with respect to the dc-link, three levels of voltage: 0 V, $-V_{bat}$, V_{bat}. The average voltage at the mid point of each of the branches a and b (so v_a and v_b) depends on the corresponding duty cycle D_1 and D_2, thus

$$v_a = V_{bat} \cdot D_1, \tag{1}$$

$$v_b = V_{bat} \cdot D_2, \tag{2}$$

Since the two sinusoidal carriers are complementary (they are shifted π rad), the duty cycles D_1 and D_2 are also complementary, thus

$$D_2 = 1 - D_1. \tag{3}$$

From above expressions, the instantaneous voltage at the AC terminals of the H-bridge can be calculated by,

$$v_{ab} = v_a - v_b = V_{bat} \cdot (1 - 2 \cdot D_2). \tag{4}$$

The voltage v_{ab} can also be renamed tov_z,

$$v_z = V_z \cdot cos(\omega \cdot t + \phi), \tag{5}$$

with V_z being the RMS value of the voltage waveform, ω the grid frequency and ϕ the grid angle. The term V_z is related to the dc-link voltage (i.e. the battery voltage) through the modulation index m as

$$m = \frac{V_z}{V_{bat}}, \tag{6}$$

so, v_z can be expressed as

$$v_z = V_{bat} \cdot m \cdot cos(\omega \cdot t + \phi). \tag{7}$$

Matching now (4) and (5), the time dependent expressions for the duty cycles D_1 and D_2 can be expressed as

$$D_1 = \frac{1}{2} + \frac{1}{2} \cdot m \cdot cos(\omega \cdot t + \phi), \tag{8}$$

$$D_2 = \frac{1}{2} - \frac{1}{2} \cdot m \cdot cos(\omega \cdot t + \phi). \tag{9}$$

The expressions above serve to compute the conduction power losses at the transistors of the H-bridge, as presented later in section 3.2.3. For calculating such losses, only the expression for D_1 is needed, as D_2 is complementary.

At this point, it is also straightforward to obtain the duty cycle for the diodes in anti-parallel disposition in the H-bridge. The duty cycle is simply the complementary for D_1, so $D' = 1 - D_1$: diodes are driving current when transistors are not.

H-bridge dc-dc converters

For H-bridge operated as a dc-dc converter, the UPWM technique is applied. It is based, as for the SPWM previously introduced, on the comparison of two carrier signals, one per converter arm, with a high frequency triangular waveform. Such comparison yields the triggering signals for transistors gate. The difference among the two techniques is that in UPWM the carriers are not sinusoidal waveforms but constant in time. As a consequence, not an ac voltage waveform is synthesized at the converter terminals but a dc waveform.

Addressing this, it is clear that the calculation of the duty cycles presented for the inverter case is not valid anymore. Duty cycle is constant in time now and depend on the magnitude of the dc voltage to be synthetized at the battery terminals with respect to the magnitude of the voltage at the dc-link and it varies between 0 and 1. Such voltage at the dc-link and the expression for duty cycle calculation is presented in the following, while addressing required voltage levels.

MMCC structures

The switching of ac-dc the modules for MMCC structures is based on the two-level SPWM technique previously presented. The difference is that the duty cycles can be calculated using different type of carriers [1], [19]. For this article, a phase-shifted SPWM strategy is employed. It consists on using a carrier per module which is shifted depending on the available modules per arm. For instance, for a n module arm, the carrier per each module is shifted $2 \cdot \pi / n$ rad. As a result of such shifting, the voltage across the arm is shared among the modules.

3.2.1.2. Voltage levels

Table 2 summarizes the voltage levels at the different interfaces between components within each PCS. For instance, for PCS #1a, the description provided in the table indicates that the voltage ratings of the dc-ac converter interfacing the battery with the coupling transformer are 400 Vdc at the battery side, and 230 Vac at the transformer side. The description also indicates that each of the power trains composing the PCS is connected to the phase-neutral terminals of the transformer.

PCS	Voltage levels (from battery pack to network connection)
#1a	Battery: 400 Vdc / dc-ac: 230 Vac (phase-neutral coupling transformer).
#1b	Battery: 400 Vdc / dc-dc: 460 Vdc / dc-ac: 230 Vac (phase-neutral coupling transformer).
#1c	Battery: 400 Vdc / dc-ac: 230 Vac / high frequency transformer ratio 1:1 / ac-dc: 400 Vdc / dc-ac: 230 Vac (phase-neutral coupling transformer).
#2a	Battery: 400 Vdc / dc-ac: 115 Vac / 2 converters in cascade yields 230 Vac per arm (phase-neutral of coupling transformer).
#2b	Battery: 400 Vdc / dc-dc: 460 Vdc / dc-ac: 115 Vac / 2 converters in cascade yields 230 Vac per arm (phase-neutral coupling transformer).
#2c	Battery: 400 Vdc / dc-ac: 230 Vac / high frequency transformer ratio 1:1 / ac-dc: 400 Vdc / dc-ac: 115 Vac / 2 converters in cascade yields 230 Vac per arm (phase-neutral of coupling transformer).
#3a	Battery: 400 Vdc / dc-ac: 200 Vac / 2 converters in cascade yields 400 Vac per arm (phase-

PCS	Voltage levels (from battery pack to network connection)
	phase coupling transformer).
#3b	Battery: 400 Vdc / dc-dc: 460 Vdc / dc-ac: 200 Vac / 2 converters in cascade yields 400 Vac per arm (phase-phase coupling transformer).
#3c	Battery: 400 Vdc / dc-ac: 230 Vac / dc-ac: 200 Vac / high frequency transformer ratio 1:1 / ac-dc: 400 Vdc / dc-ac: 200 Vac / 2 converters in cascade yields 400 Vac per arm (phase-phase coupling transformer).
#4a	Battery: 400 Vdc / dc-ac: 230 Vac (phase-neutral point of each star).
#4b	Battery: 400 Vdc / dc-dc: 460 Vdc / dc-ac: 230 (phase-neutral point of each star).
#4c	Battery: 400 Vdc / dc-ac: 230 Vac / high frequency transformer ratio 1:1 / ac-dc: 400 Vdc / dc-ac: 230 Vac (phase-neutral point of each star).
#5a	Battery: 400 Vdc / dc-dc: 460 Vdc / 6 converters in cascade yields 2760 Vdc / 3-phase dc-ac: 400 Vac (phase-phase coupling transformer).
#5c	Battery: 400 Vdc / dc-ac: 230 Vac / high frequency transformer ratio 1:1 / ac-dc: 400 Vdc / 6 converters in cascade yields 2400 Vdc / 3-phase dc-ac: 400 Vac (phase-phase coupling transformer).
#6a	Battery: 400 Vdc / dc-dc: 800 Vdc / 3-phase dc-ac: 400 Vac (phase-phase coupling transformer).
#6c	Battery: 400 Vdc / dc-ac: 230 Vac / high frequency transformer ratio 1:1 / ac-dc: 800 Vdc / 3-phase dc-ac: 400 Vac (phase-phase coupling transformer).

Table 2: Voltage levels for each PCS.

As noted in Table 2, given the rated voltage of 400 V for battery packs, the voltage level at the opposite side of dc-dc converters directly interfacing with batteries is set at 460 V. The calculation of such value is presented in the following.

The voltage at the above mentioned point, and according to the assumptions in subsection 3.2.1, should be set as the minimum required one for maximum performance. The minimum required dc-link voltage can be deduced from the case a unitary duty cycle is to be applied. Maximum duty cycle (D_{max}) is for the case the battery voltage is also maximum and it is still being charged at nominal current. Under these operating conditions, and considering the voltage drops at the inductive filter interfacing the converter and the battery, as well as those at the switches, the minimum required voltage at the dc-link of the converter can be calculated as

$$V_{dc} \geq \frac{I \cdot \left(2 \cdot r_{ce} + r_l + r_s \cdot \frac{n_s}{n_p}\right) + 2 \cdot V_{ce} + V_{bat_{eoc}}}{2 \cdot D_{max} - 1}, \tag{10}$$

being I the nominal current through the battery pack, calculated as $I = P_{bat}/V_{bat}$; r_{ce} the internal resistance of the transistors and V_{ce} the corresponding voltage drop; n_s and n_p the number of cells in series and in parallel configuring the battery pack; r_s the internal resistance of battery cells; and $V_{bat_{eoc}}$ the voltage of a battery cell at the end-of-charge condition, which can be calculated by the product of $V_{cell_{eoc}}$ and n_s.

Once the minimum required dc-link voltage is calculated, the duty cycle to be applied by the converter while charging the battery at nominal operating conditions (both in current and voltage for the battery pack), can be easily computed by

$$D = \frac{1}{2}\left(1 + \frac{I \cdot \left(2 \cdot r_{ce} + r_l + r_s \cdot \frac{n_s}{n_p}\right) + 2 \cdot V_{ce} + V_{bat}}{V_{dc}}\right). \quad (11)$$

Finally, just include some notes on the voltages presented in the Table around the ac voltage synthetized by the inverters directly interfacing with battery packs. Such voltage is 230 Vac, which means that the modulation factor to be applied by the inverter is $m = 230 \cdot \sqrt{2}/\,400 = 0.810$. This modulation factor ensures a safety operating point for the inverter while it is high enough to ensure the proper utilization of inverter capabilities.

3.2.2. Discussion on reliability

The term reliability refers to the ability of a system or component to perform its required functions under stated conditions for a specified period of time [32]. A way to estimate the reliability of a system is calculating the so-called mean-time between failures (MTBF). This metric is typically expressed in hours. In general terms, the higher the MTBF, the higher the reliability of a product is.

Using the parts count prediction method, included in the MIL-HDBK 217, the failure rate for a component or system λ (usually expressed in failures / 10^6 hours) can be computed by

$$\lambda = \sum_{i=1}^{n} N_i \cdot \left(\lambda_g \cdot \pi_Q\right)_i, \quad (12)$$

where λ_g is the generic failure rate for the i^{th} generic part, expressed in [failures / 10^6 hours]; π_Q is the corresponding quality factor; N_i is the quantity of the i^{th} generic part; and n is the number of different parts in the component or system being evaluated.

For electronic systems, in which unlike mechanical ones there are not moving parts, it is generally accepted a constant failure rates during the useful operating life. Doing this, the predicted reliability for a component or system at specific operating life in hours $R(t)$, can be computed by

$$R(t) = e^{-\lambda \cdot t}, \quad (13)$$

and is expressed in per unit adopting values between 0 and 1. As noted, reliability function presents an exponential shape.

Method MIL-HDBK-217F offers a data base for electronic components [55]. Assuming quality factor $\pi_Q = 1$ in all cases, the typical failure rate λ for the main components building up the different PCSs to be evaluated are: $\lambda_{Mosfet} = 1.1 \cdot 10^{-9}$ failures / hour for MOSFETs; $\lambda_{Diode} = 7.5 \cdot 10^{-9}$ failures / hour for diodes; $\lambda_{Inductor} = 2.0 \cdot 10^{-10}$ failures / hour for an inductor; $\lambda_{Capac} = 2.5 \cdot 10^{-9}$ failures / hour for a capacitor; $\lambda_{LF-tr} = 3.6 \cdot 10^{-7}$ failures / hour for a low frequency transformer; $\lambda_{HF-tr} = 9.6 \cdot 10^{-7}$ failures / hour for a high frequency transformer. From the failure rate of individual components and using equation (12), the failure rate for the ac/dc and dc-dc H-bridge, as well as for 3 phase H-bridge inverter results: $\lambda_{bridge} = 3.4 \cdot 10^{-8}$ failures / hour for the ac/dc and dc/dc H-bridge; and $\lambda_{3-bridge} = 5.2 \cdot 10^{-8}$ failures / hour for the 3 phase bridge. Finally, the typical failure rate for a battery pack is assumed as $\lambda_{bat} = 1.0 \cdot 10^{-5}$ failures / hour.

Now, applying equation (13), and for a lifespan of 50000 hours (5.7 years), the reliability for each of the above components is: 0.999945 for MOSFETs; 0.999625 for diodes; 0.999990 for an inductor; 0.999875 for a capacitor; 0.982161 for a low frequency transformer; 0.953133 for a

high frequency transformer; 0.998281 for the ac/dc and dc/dc H-bridge; 0.997423 for the 3 phase bridge; and 0.606530 for a battery pack.

Once the reliability of each individual component is calculated, one can calculate the reliability of each of the proposed PCS. To do so, the reliability block diagram method is adopted [12]. This method permits to estimate the reliability of a system in which blocks (or components) are connected in series and/or parallel. For block connected in series, the associated reliability becomes

$$R_{series} = \prod_{i=1}^{n} R_i, \tag{14}$$

while for blocks in parallel, it becomes

$$R_{parallel} = 1 - \prod_{i=1}^{n} (1 - R_i). \tag{15}$$

Applying the algebra above, the reliability of each of the proposed PCSs can be calculated. Results are presented in Table 3. For the sake of clarity, and as an example, the reliability block diagram for PCS #6 is presented in Figure 3. The block diagrams for the rest of the PCSs (variant a)) are included in the Appendix.

	Variants at module level		
Identifier	**(a) 1 conversion step**	**(b) 2 conversion step**	**(c) with galvanic isolation**
#1	0.996225	0.996160	0.994105
#2	0.745779	0.744150	0.700043
#3	0.745779	0.744150	0.700043
#4	0.996225	0.996160	0.994105
#5	0.049103	-	0.036437
#6	0.993524	-	0.991498

Table 3: Estimation of reliability for the PCSs.

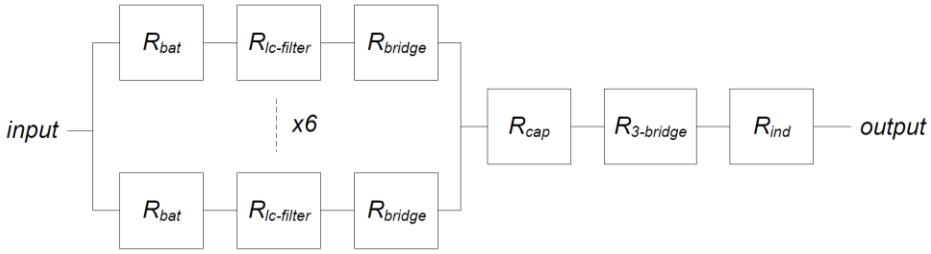

Figure 3: Reliability block diagram for PCS \#6 variant (a).

From Figure 3, the mathematical function for reliability calculation of PCS #6 variant (a) is

$$R_{PCS6a} = R_{ind} \cdot R_{3-bridge} \cdot R_{cap} \cdot \left(1 - \left(1 - R_{bat} \cdot R_{lc-filter} \cdot R_{bridge}\right)^6\right). \quad (16)$$

From the results in Table 3, it can be observed that PCS #1, in all proposed variants, is intended as the most reliable one. This is, in fact, one of the reasons because this topology has been actually built and installed in field. By parallelizing diverse power trains, the failure in one of them does not necessarily provoke the interruption of the whole system. Under such circumstance, the ac terminals of the power train affected by the eventuality could be easily disconnected from the rest of the system through a conventional low voltage breaker.

With the same expected reliability of PCS #1 we have the PCS #4 (an MMCC double star topology). Given 6 battery packs, the double-star concerns just one block per each arm. At the end, the double star configures six blocks connected in parallel, so with the same reliability of PCS #1. However, the way of managing the PCS #4 is more complicated than for PCS #1 in case of an eventuality in one of the battery modules. For instance, if one of the converter arms fails, the entire phase unit operation is disabled. The PCS could still be operated under bipolar mode though.

Anyhow, despite the challenging management of MMCCs, and also in regard of a comparison of reliability for PCS #1 and #4, [70] concludes that the reliability of the latter is even higher than for the PCS #1 till reaching loading rates up to 93% with respect to the ratings of the particular system considered in this work. The reason supporting this conclusion is that for very high loading rates, all modules of the MMCC should work (there are no modules in idle mode anymore) so a failure of one of them can be critical, thus sensibly lowering the reliability of the whole system.

Immediately below PCS #1 and #4 in reliability, we find PCS #6. Either in variant (a) or (c), the connection of battery modules in parallel yields a very high reliability. The little difference with PCS #1 (the topology with maximum reliability) is because of the fact that an eventuality in the 3-phase grid side inverter would disable the whole PCS.

Further, with a sensibly lower reliability than for PCS #1, we find PCSs #2 and #3. These topologies (MMCC in star and delta configurations) offer interesting features. Given 6 battery packs, these are distributed in pairs, one pair per arm, which is then directly connected to the grid connection point. At the end, in both star and delta configurations, three strings of batteries (i.e. two battery packs in series) are seen in parallel configuration from the point of view of the network, so an eventuality in one battery pack would disable one arm (i.e. two battery packs), letting the other two ones still available, so 67% of the rated power still in operation.

Finally, PCS #5 present the lowest reliability among eligible. The connection of all battery packs in series and the need of interacting with the main grid through a single 3-phase inverter, make this topology as barely reliable. The obtained value for reliability (e.g. 0.049103 for variant (a)) means that the probability of experiencing a failure disabling the whole PCS during the 50.000 hours of expected lifespan is very high.

3.2.3. Discussion on efficiency

Assessing the efficiency of each of the PCSs under discussion is a challenging task. The efficiency depends on the number of power converters included in each PCS, their voltage and current ratings, and the way they are connected between each other and operated (switching techniques). The aim of the following lines is just to provide rough estimations making the comparisons as fairer as possible. To do so, the assumptions presented at the beginning of section 3.2.1 are adopted. An additional assumption is that for efficiency calculations, the following losses are to be considered: i) those in the transistors (both conduction and switching ones) configuring the H-bridge converters or modules building up the PCSs; ii) those associated

to battery packs; iii) and those associated to high-frequency transformers. Thus, losses in passive components are not addressed, since these are not --but the losses in the transistors-- what mostly determine the efficiency of the modules.

The first step to assess the efficiency is to present a common methodology. Similar to the assessment of reliability in section 3.2.2, the efficiency of each PCS is based on mathematical expressions built up from the particular efficiency of each module, all configuring efficiency block diagrams. So, for instance, the efficiency block diagram for PCS #6 (variant (a)), is plotted in Figure 4. This block diagram also applies for PCS #5 variant (a).

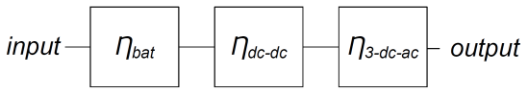

Figure 4: Efficiency block diagram for PCS #6 variant (a). This block diagram also applies for PCS #5 variant (a).

As can be noted, the efficiency of the whole PCS #6 variant (a) can be simply resembled to the efficiency of one of the 6 power trains comprised by the series connection of a battery pack and a dc-dc conversion step, all connected to the front-end dc-ac converter. The efficiency is calculated considering the case the battery is being discharged. Similar results will be obtained by considering a reversal power flow. From Figure 4, the efficiency is calculated by the product of the particular efficiency of the different elements connected the way described above, so

$$\eta_{PCS6a} = \eta_{bat} \cdot \eta_{dc-dc} \cdot \eta_{3-dc-ac} \quad , \tag{17}$$

being η_{PCS6a} the efficiency of the whole PCS, η_{bat} the efficiency of a battery pack, η_{dc-dc} the efficiency of the H-bridge working as a dc-dc converter, and $\eta_{3-dc-ac}$ the efficiency for a three-phase H-bridge inverter.

For the sake of completeness, the block diagrams for the rest of PCSs considered in this work (variant (a)), as well as the corresponding mathematical expressions for efficiency calculations, are presented in the Appendix.

As previously introduced, the accuracy for the estimation of the efficiency of the different PCSs relies on the estimations for the efficiency of particular components (batteries, H-bridges and so on) and these depend on the operating conditions (see subsection 3.2.1).

The power converters building up the different PCSs are all based on H-bridges, either one-phase or three-phase ones, operated under SPWM or UPWM switching schemes. Following contents describe the formulas for switching and conduction power losses calculation of the transistors (and corresponding diodes in anti-parallel disposition) under above mentioned switching schemes.

3.2.3.1. H-bridge ac-dc converter

Once the duty cycle D is known, the conduction power losses for a transistor can be calculated by

$$P_{tr-c} = \frac{2}{\pi}\int_0^{\frac{\pi}{2}} (v_{ce} \cdot i \cdot D)\, d\theta, \tag{18}$$

being i the current actually exchanged with the grid and v_{ce} the collector emitter voltage drop at the transistor. The current i can be expressed as

$$i = \sqrt{2} \cdot I \cdot cos(\theta). \tag{19}$$

The voltage v_{ce} can be shaped to a curve depending on the current i in the form of

$$v_{ce} = U_0 + r \cdot i^b, \tag{20}$$

being U_0, r and b shaping parameters deduced from the datasheet provided by transistors' manufacturer.

The calculation of the conduction power losses for a diode P_{di-c} can be calculated analogously, just replacing D by D' and the new expression for v_{ce} considering the diode characteristics.

The switching power losses for a transistor does not depend on the duty cycle but on the switching frequency along with the energy lost in one turn-on and turn-off event during a period. These energies can be associated to from mathematical functions shaping the curves provided by manufacturers in their datasheets. These curves are depending on the driving current I (RMS value) through the transistor. For the energy lost while turning on, for instance, this function can have the form of

$$E'_{on} = \frac{I^k}{\beta}, \tag{21}$$

being k and β the shaping parameters.

The curves provided by manufacturers are usually expressed considering standard dc-voltage voltage across the transistor, named as V_{cc}. In the present case this is V_{bat}, so E'_{on} can be corrected by

$$E_{on} = E'_{on} \cdot \frac{V_{bat}}{V_{cc}}. \tag{22}$$

Using now the expression for E_{on} (and that analogously proposed for E_{off}), the power losses for a transistor for a switching period is

$$P_{tr-sw} = \frac{1}{\pi}\int_0^{\frac{\pi}{2}} \left(E_{on} + E_{off}\right) \cdot f_c \cdot d\theta, \tag{23}$$

being f_c the switching frequency in Hertz.

The switching power losses for a diode can be calculated adopting an analogous procedure than for transistors. Here, manufacturers are providing information for the turn-off process, because it is when losses are incurred. For that situation, energy lost is named as E_{rr} and the expression for power losses calculation is

$$P_{di-sw} = \frac{1}{\pi}\int_0^{\frac{\pi}{2}} E_{rr} \cdot f_c \cdot d\theta, \tag{24}$$

From above expressions, the total power losses for a H-bridge operated as an inverter are given by

$$P_{ac-dc} = 4 \cdot (P_{tr-sw} + P_{di-sw}) + 4 \cdot (P_{tr-c} + P_{di-c}). \tag{25}$$

In turn, the efficiency is expressed as

$$\eta_{ac-dc} = 1 - \frac{P_{ac-dc}}{P_{bat}}, \tag{26}$$

being P_{bat} the power provided by the battery pack.

3.2.3.2. H-bridge dc-dc converter

The expressions for power losses calculation previously introduced can be essentially used for a H-bridge operated as a dc-dc converter under the UPWM switching technique. Some changes should be applied though and these are introduced in the following.

Given the duty cycle D and current I as calculated above, the expressions for power losses in transistors can be directly adopted. In dc-dc operating mode, diodes are never driving so there are no losses incurred in them and total power losses in the converter are given by

$$P_{dc-dc} = 4 \cdot (P_{tr-sw} + P_{tr-c}) \tag{27}$$

Once the methodology for efficiency calculation has been presented, following contents address the efficiency comparison among PCSs. Previously though, some required notes introduced around the efficiency of the battery packs and the high frequency transformer. The efficiency of these components are considered as constant for all PCSs since the operating conditions are the same for all cases. The efficiency for both low and high frequency transformers is very high. For low frequency transformers, it typically reaches --and even exceeds-- 99% for medium-sized (tens of kVA) transformers. The efficiency of high-frequency ones could result increased because core losses are function of frequency (see Steinmetz equation [82]). On the other hand though, the core materials utilized in high frequency transformers have a hysteresis cycle much more narrow than that for the materials in low frequency transformers. At the end, the efficiency of high frequency transformers can result as high as for low frequency ones. As a figure of merit, in this work an efficiency of 99% is also assumed for this type of transformers. In regard of battery packs, an efficiency around 97% is assumed. Finally, adopting the efficiency block diagrams along with the methodology and assumptions for efficiency estimation of the different components, the efficiency of the different PCSs proposed in this work are summarized in Table 4.

	Variants at module level		
Identifier	**(a) 1 conversion step**	**(b) 2 conversion step**	**(c) with galvanic isolation**
#1	0.935	0.910	0.860
#2	0.902	0.876	0.830
#3	0.931	0.909	0.856
#4	0.935	0.910	0.860
#5	0.898	-	0.850
#6	0.923	-	0.867

Table 4: Comparison on energy efficiency for the proposed power conversion systems.

Table 4 clearly states that the efficiency reduces along with the complexity of the PCSs. This is obvious while comparing, for instance, PCS #1 variant (a) with variants (b) and (c): the higher the number of components building up each of the power trains of the PCS is, the lower the expected efficiency.

Now comparing the efficiency among PCSs (just variants (a) and (b)), it can be deduced that the PCSs with the highest efficiency are the number #1 and #4. For variant (a), efficiency reaches the value of 0.935 p.u., while it is expected at 0.910 for variant (b). The parallel connection of power trains with the network coupling point in these topologies results into maximum efficiency. This is one of the reasons supporting the wide implementation of PCS #1 by industry. According to the assumptions of the present work, PCS #4 results as efficient as PCS #1. However, this is because of the reduced number of modules composing the PCS. For large number of modules, in which some are connected in cascade in each of the arms of the PCS, the efficiency is expected to be lower than for PCS #1.

Anyhow, after PCSs #1 and #4, PCS #6 is identified as the most interesting one in terms of efficiency. For variant (a), the efficiency (0.923 p.u.) is quite similar to the efficiency for PCS #1. For variant (c), PCS #6 is even the best one among eligible. The parallel connection of dc-dc conversion steps to a common dc-link is thus identified as a promising option in terms of efficiency.

Then, with an efficiency of about 0.931 and 0.902 p.u. (variant (a)) we find PCSs #3 and #4 respectively. These PCSs are based on MMC topologies. The factor $\sqrt{3}$ affecting the current through the different modules in star configuration (PCS #3); and the voltage across the modules in delta configuration (PCS #4) respectively, yield a slightly lower efficiency for these PCSs in comparison to PCS #1.

Finally, with the poorest efficiency among eligible, we find PCS #5. Definitely, the configuration of dc-dc conversion steps in cascade is not convenient in terms of efficiency. The resultant dc voltage between the terminals of the cascaded association is high, yielding remarkable losses at the front-end inverter of the PCS.

3.2.4. Discussion on fault tolerance

The fast expansion of power electronics and renewable energies has propitiated the development of sustainable transportation and power systems. As the number of power converters and, consequently, the number of interconnections between the utilities and different storage systems is increasing day by day, the fault tolerances topic is at the centre of things.

Several causes located at different locations can cause critical faults on some part of the electric conversion. Thus, the relevant parts to focus on fault tolerance topic are the converter itself (internal faults), and the cables (dc or ac).

On one hand, internal faults involve possible semiconductor faults such as short-circuit due to a bad behaviour of a switch or an incorrect trigger signal. This situation is usually saved by specific hardware depending on the applied technology. Different solutions aims to protect the system permitting to block the semiconductor in a safe way. An example is to add a soft turn-off circuitry to the driver that manages the semiconductors. Thus, soft turn-off can be used for decreasing the turn-off voltage overshoots over the semiconductor switch when high currents are involved, avoiding a damage to the converter.

On the other hand, many authors are recently addressing the fault analysis hot topic applied to DC network cables and their dynamic effect [40]. As cited in [43], conventional converters (voltage source converters and MMCCs) are not able to isolate DC faults by themselves. These converters are vulnerable to dc-cable short-circuit and ground faults due to the high discharge current from the dc-link capacitance [98], being the most sensitive situation the pole-to-pole fault [43]. In fact, as detailed in [43], in some topologies like PCS #4, fault currents at the DC side, AC wires and in the converter exist all time, even after blocking the sub-modules of an arm phase. This is due to the behaviour as an uncontrolled rectifier. All these situations suppose that the fault located at the DC cabling should be isolated by additional devices. Some of the used

alternatives are fast cutting-edge DC breakers [57], [102], modified AC breakers combined with fast static switches [84] or by means of modified converter sub-module units [14].

However, in the case of PCSs for modular battery-based energy storage systems a DC fault can be assumed as rare due the proximity between the storage system and the converter itself. In this sense, for the study case, the fault tolerance analysis is concentrated on the AC side fault. Some other authors, as [44], also attends to this kind of faults instead of DC ones. Actually, a wall bushing insulation fault is proposed by [44] as a probable source of AC faults. In that sense, and according to the different PCS topologies presented in Figure 2, a three-phase minimal conversion unit is hereinafter adopted for comparison of fault tolerance. Figure 5 depicts in blue those minimal units connected to the utility per each PCS case. Conforming to this, PCS #1 will be the minimal unit reference. For the reference PCS (i.e. PCS #1), each connected battery pack voltage is U V, the PCS exchanges a power of S VA, can synthesize a phase-to-phase AC voltage of V V, and is interfaced with the grid by means of a type-L filter, for simplicity.

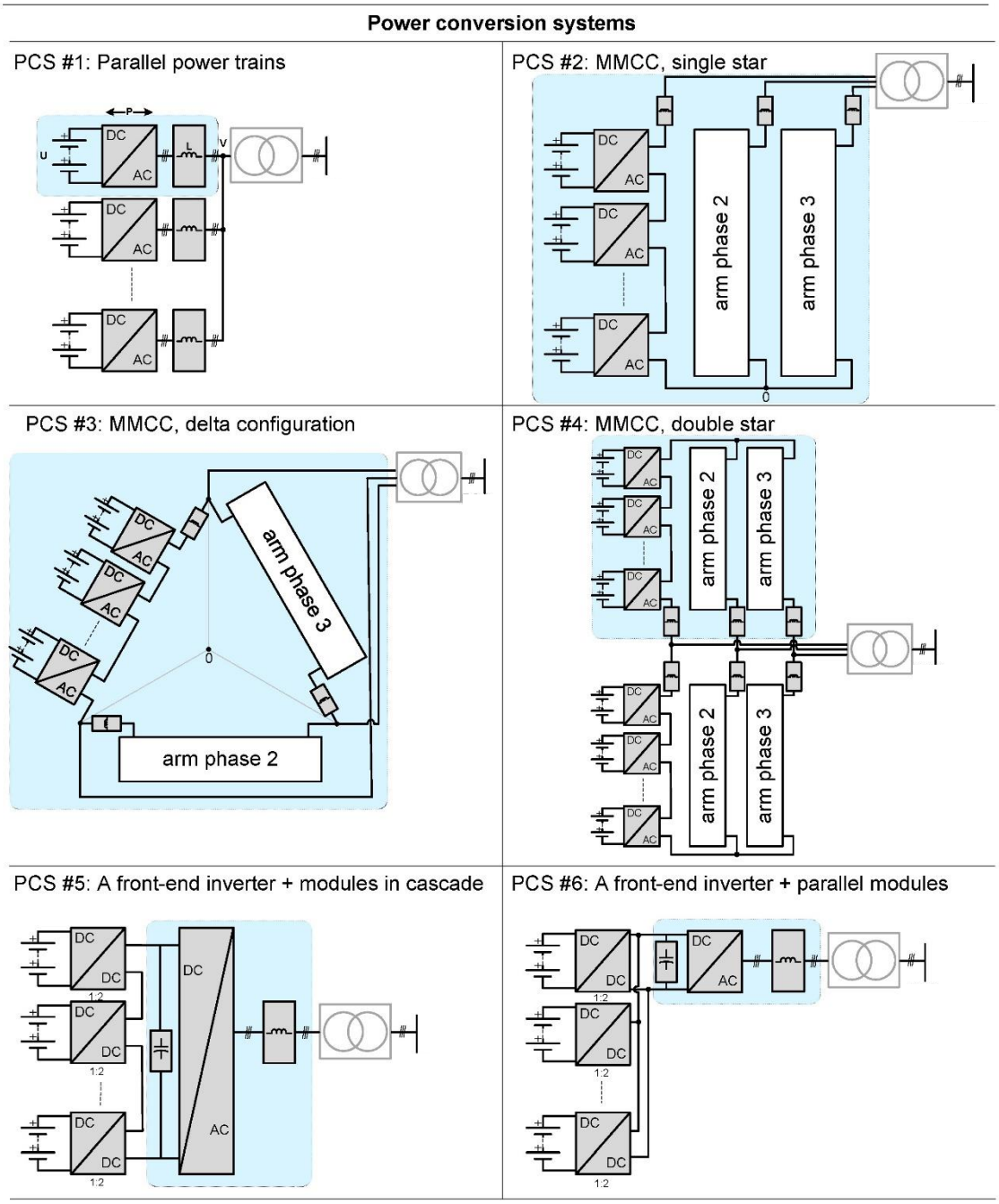

Figure 5: PCSs for modular battery-based energy storage systems highlighting in blue the minimal three-phase power unit connected to grid.

Following this criteria, Table 5 shows seven values of comparison; maximum phase-to-phase AC side synthesizable voltage (V_g), exchanged power (P), rated AC filter current (I_r), employed modulation technique, effective switching frequency and voltage drop that the type-L filter has at its terminals (ΔU and f_e) and, finally, the self-inductance value (L). It should be noted that the modulation technique has been selected according to two possible situations. If the dc-ac involves a three-phase inverter it is assumed Space Vector PWM for maximum profit of the dc-link voltage (case of PCS #1, #5 and #6). If the DC/AC involves an arm-phase sub-module of a MMCC it assumed unipolar modulation for optimal design in terms of output current ripple (case of PCS #2, #3 and #4). Also, in case of DC/DC power stages involved, a 1:2 voltage ratio is assumed (case of PCS #5 and #4). Finally, each full PCS by a total of six conversion systems.

Identifier	V_g	P_r	l_r	Modulation	ΔU	f_e	L
PCS #1	V	S	I	SPWM	U	f	L
PCS #2	4·V	6·S	(3/2)·I	UPWM	U/2	2·f	L/6
PCS #3	2·V	6·S	$(\sqrt{3})$·I	UPWM	U/2	2·f	L/(4·$\sqrt{3}$)
PCS #4[1]	2·V	3·S	(3/2)·I	UPWM	U/2	2·f	L/3
PCS #5[2]	12·V	6·S	I/2	SPWM	12·U	f	24·L
PCS #6[2]	2·V	6·S	3·I	SPWM	2·U	f	(2/3)·L

[1] The self-inductance is assumed to be splitted between top and bottom arms of each phase.
[2] Assuming that level of exchanged power in respect with PCS #1 should imply lower switching frequencies in real devices. Here, it is maintained the frequency for better understanding.

Table 5: Fault tolerance comparison according to minimal connected unit per each PCS topology.

Once the values of Table 5 are obtained a common value for all PCS can be computed as an index to evaluate a PCSs fault tolerance. The adopted index is the ratio di/dt over I_r when a fault in the grid terminals appears. This index is named FTI (Fault Tolerance Index). The computation of the FTI for the different PCS minimal AC units can be seen in Table 6, assuming FTI in PCS #1 as the reference and equal to 1. The higher the FTI the lower the fault tolerance. In general terms, it can be deduced that MMCC are less fault tolerant to an AC fault.

Identifier	FTI
PCS #1	1
PCS #2	16
PCS #3	8
PCS #4	4
PCS #5	1
PCS #6	1

Table 6: Fault Tolerance Index (FTI).

3.2.5. Discussion on compactness

A straightforward method to assess compactness could be through components counting. To make this counting as fair as possible, a weighted sum is proposed, and weighted coefficients are depending on the power the power density, which are multiplied by the rated power of each of the components' type. At the end of the day, the total volume for a PCS i, V_i, will be calculated by

$$V_i = \int_{j=1}^{J} n_j \cdot P_j \cdot \alpha_j^{-1}, \qquad \forall\, i \backslash in\, I, \tag{28}$$

being I the set of PCSs to evaluate; J is the number of components' type in each of the PCSs; n_j is the number of times each of the components' type appears in each of the PCSs; P_j the rated power of the component; and α_j the weighted coefficient for each of the components' type.

The weighting coefficients (the power densities, in fact) are considered as typical values from commercial systems and the experience of the authors of the present work. These are presented in the following:

- α_{LF-tr} for a low frequency transformer. This is assumed as 68 kVA/m^3. This is a typical power density for a three phase 30 kVA / 50 Hz transformer by one of the principal manufacturers [22].
- α_{HF-tr} for a high frequency transformer. This is assumed as 7395 kVA/m^3. This is derived from the characteristics of a commercial single phase transformer of 4 kVA approximately, working at frequencies between 20 and 50 kHz and at voltages around 150 Vac [71].
- α_{mod} for an ac-dc or dc-dc module based on H-bridges. This is assumed as 215 kVA/m^3. This is derived from the characteristics of a commercial transformerless ac-dc inverter rated at 30 kW / 480 Vac [15].
- α_{bat} for a battery pack. This is assumed as 362 kWh/m^3, being obtained as detailed in the following. Firstly, note that the pack is based on 10 strings of 108 lithium-ion cells in series each. So, addressing the dimensions of a 18650 lithium ion cell (18 mm diameter times 65 mm height), and oversizing the pack 10% in volume for battery management system and ancillaries, the volume of a 10 kWh pack is estimated as 0.027 m^3. From this value the energy density indicated above can be easily calculated.

Applying the above formula and parameters to all considered PCSs, volumes can be calculated. The adopted assumptions for calculation are the same as for the rest of the work, i.e. each battery pack is rated at 4.8 kWh; each corresponding power conversion module is rated at 5 kVA; and for PCS #5 and #6 the front end inverter is rated at 30 kVA. Results are presented in Table 7. Three main aspects are listed in the following:

- The estimated volume for variant (a) for PCSs #1 through #4 are equal, as well as that for variant (b) and (c). For variant (a), estimated volume is 0.740 m^3; 0.878 m^3 for variant (b); and 1.020 m^3 for variant (c). So the differences are not among PCSs, but among variants. This is because the above PCSs have the same number of battery packs, power modules and transformers (e.g. PCS #1 variant (a) has 6 power modules, 6 battery packs and 1 low frequency transformer, and this is also for PCS #2 variant (a)). So for PCSs #1 through #4, adopting the most complex variant (variant (c)), is translated into an increment in expected volume of nearly 40% with respect to the volume of the simplest variant (variant (a)).
- Similarly, the estimated volume for variant (a) for PCSs #5 and #6 are equal, as well as that for variant (c). For variant (a), estimated volume is 0.878 m^3, while it is 1.020 m^3 for variant (c). So for these PCSs, adopting the most complex variant (variant (c)), is translated into an increment in expected volume of about 17% with respect to variant (a).
- To sum up, and addressing now all PCSs at once, it is worth noting that any of them are assumed as impractical for excessive volume in comparison to the rest of the alternatives. Also, it is worth noting a non-excessive increment (40% at most) while adopting the most complex variant with respect to variant (a).

	Variants at module level		
Identifier	**(a) 1 conversion step**	**(b) 2 conversion step**	**(c) with galvanic isolation**
#1	0.740	0.878	1.020
#2	0.740	0.878	1.020
#3	0.740	0.878	1.020
#4	0.740	0.878	1.020
#5	0.878	-	1.020
#6	0.878	-	1.020

Table 7: Estimation of volume for the PCSs.

3.2.6. Discussion on flexibility

This section proposes a discussion on the flexibility of the PCSs. The term flexibility is intended here as the ability to manage a PCS in different operational circumstances. Circumstances, for instance, such as the connection of batteries of different type in the diverse modules of the PCS. The inclusion of batteries with different voltage levels and characteristics (state-of-charge, admissible current rates, cycling, and etcetera) challenges the operation and stability of the PCSs and this is topology dependent. Another circumstance can be the connection of the PCS to a weak grid, so the focus should be on power quality issues such as harmonics and power unbalances. Further even, another circumstance can be the need of balancing the state-of-charge of the different batteries connected in the diverse modules of the PCS. Altogether yields the flexibility as an important feature for a modular PCS, and this is briefly addressed in the following lines.

In general terms, and among considered options, the PCS #1, is the most flexible one. A proof of the high flexibility of this topology is the fact that this option is recurrently adopted by the industry, as noted in Table 1. The parallel connection of different power trains to a common point with the external grid maximizes its flexibility. The batteries connected at the different power trains can be of diverse voltage, energy and power ratings, since the interaction between the power trains is minimum and these can be managed almost independently. One drawback of this PCS in regard of flexibility is that because of its high cost --each power train comprises a dedicated front-end inverter--, designers may consider the reduction of the number of power trains thus configuring large battery packs to fulfil the energy storage requirements. The variations of the voltage and internal impedance of battery packs with large number of cells in series and in parallel can affect the stability of the PCS in connection with the external grid, as addressed in [7], [47].

The flexibility for PCSs #2 and PCS #3 propose the connection different modules in cascade, and this poses challenges from an operational point of view. Such challenges are addressed in [92], where the operation of the converter under unbalanced grid conditions. Firstly, the work concludes that the operation of such PCSs under grid unbalances is more challenging that for conventional three-phase topologies (e.g. PCS #1), since each of the PCS branch (either in star or delta configuration) is affected in different manner and thus, has to be operated differently. To facilitate this operation, the work also concludes that it is very convenient to opt for two conversion steps at module level (i.e. adoption of variant (b)). The second conversion step (i.e. the dc-dc converter interfacing with the battery terminals), avoids the transfer of harmonic currents experienced by the dc-link capacitor of the dc-ac H-bridge converter of the module. This is particularly important in the case of star connection (PCS #2). Under this configuration, the three arms of the PCS should generate the three-phase system sinusoidal voltage and current. This directly yields power fluctuations in the arms of double the grid frequency, so second order current harmonics flow through the dc-link capacitors of dc-ac modules in variant

(a). These would be directly experienced by batteries without the inclusion of a second dc-dc conversion step [5], so such second conversion step is beneficial for the battery packs in regard of an extended lifetime. The second benefit from opting for variant (b) is related to the enhanced controllability of the state-of-charge of the different battery pack splitted throughout the PCS, as also addressed in [88].

The flexibility of PCS #2 is further investigated in [72], now considering batteries of different voltage at each of the modules of the PCS. The work highlights the possibility of doing so with this topology --not addressing though the difficulties identified above and derived from connecting in cascade different modules--. The work indicates the possibility of reducing the number of modules while considering some of them with increased battery voltages, and also of applying different switching techniques --advanced ones-- at each module (e.g. high-frequency PWM for one cell and low-frequency switching rates at the others, as proposed in [52].)

Finally, also in regard of PCSs #2 and #3, just note that flexibility for variant (c) could be affected by the relatively narrow voltage conversion gain of the module, so this could be a constraint while applying batteries of different voltage. The voltage conversion gain is partly determined in this case by the high-frequency transformer with fixed transformation ratio [76].

The flexibility of PCS #4 is investigated in diverse literature [90] and [70]. In [90] flexibility is addressed by investigating power balancing algorithms among the different modules of the MMCC. Provided that the number of modules in each of the arms of the converter is large --even including reserve modules--, the possibility of applying sorting strategies for the modules while switching is one of the key features of this type of PCSs. Power balancing algorithms permit to balance the state-of-charge among batteries while still having modules in cascade, as for PCSs #2 and #3. The importance of such power balancing algorithms is not only identified as a performance of PCSs based on MMCC but as a necessity, highlighting the challenging control of this type of PCSs. For instance, as reported in [70], even with the same number of modules turned-on, the inclusion of batteries of different voltage at the different modules, may lead to uncontrolled currents flowing through the arms of the converter, thus creating additional losses and harmonics. Power balancing algorithms are of principal importance to turn such circulating currents not as a problem, but as a way to let modules to exchange power between each other yielding a balanced structure [103].

Around the flexibility of PCS #5, remarkable issues are derived from the cascade connection of the different modules interfacing the battery packs with the front-end inverter. By connecting the batteries in cascade, the capacity of the association (in Ah) is limited to the capacity of the weakest battery pack, since the net charging or discharging current provided by the whole association flows through each battery pack. So, to maximize the available energy capacity of the association, power balancing control mechanisms should be included. This aspect is addressed in [63]. The authors proposes a control structure for the modules in cascade in which each one is controlled through two control loops. The inner loop manages the current exchanged by the corresponding battery pack enabling power sharing with the rest of the packs or modules. The control reference for the inner current control loop is determined by an outer (and slower) voltage control loop. This current control loop reference needs to be dynamically varied with respect to battery parameters and, as a result, the bandwidth for the control loops of the different modules can sensibly vary, thus affecting the interoperability of the cascaded association. Among the conclusions of the work, the authors claim that a control system based on conventional proportional-integral controllers in cascade cannot guarantee the stability of the system in all operating conditions. Problems arise specially at the end of charging and discharging cycles, eventually provoking inadvertent tripping in the converter. The problem addressed above is exacerbated while considering the inclusion of battery packs of different characteristics, as considered in [61]. There, the setpoints for the voltage and current control loops for the modules are derived from an optimization problem.

Finally, PCS #6 (as PCS #1) is identified as a PCS with maximum flexibility. Here, in each power train, the dc/dc power conversion stage interfacing the battery pack terminals with the dc-link of the front-end inverter controls the charge and discharge profiles of the batteries. Since parallelized, each dc/dc converter of each power train can perform different charge and

discharge profiles following the instructions of an energy management system. So, no modules in cascade are limiting and/or affecting the capabilities of the whole system.

3.3. Comparison synthesis

Based on the different exercises comparing PCSs in the previous section 3.2, following contents remark the most important aspects:

- PCS #1 through its different variants, is identified as the most convenient option addressing all criteria considered in this work. This is reliable, efficient, flexible, compact, as well as it offers good performance under faults.
- PCS #6 follows PCS #1 in most of the criteria considered in this work. Thus, it is considered also as a good candidate for modular battery based solutions, with the potential of even improve the performance of PCS #1, by using less power converters.
- MMCC structures, as those considered in PCS #2 through #4, are identified as promising options in the future. Research and development should concentrate here in the development of power sharing algorithms that ensure the balance of charge among the different battery packs. This would permit to overcome the drawbacks of connecting in cascade different battery packs.
- Finally, PCS #5 is identified as the weakest configuration among eligible. The connection of different battery packs in cascade, configuring a medium voltage dc-link that is to be managed by a single three-phase front-end inverter, is identified as a hardly reliable option, as well as poorly flexible and efficient one.

Complementing such conclusions, Figure 6 offers a graphical comparison synthesis among PCSs.

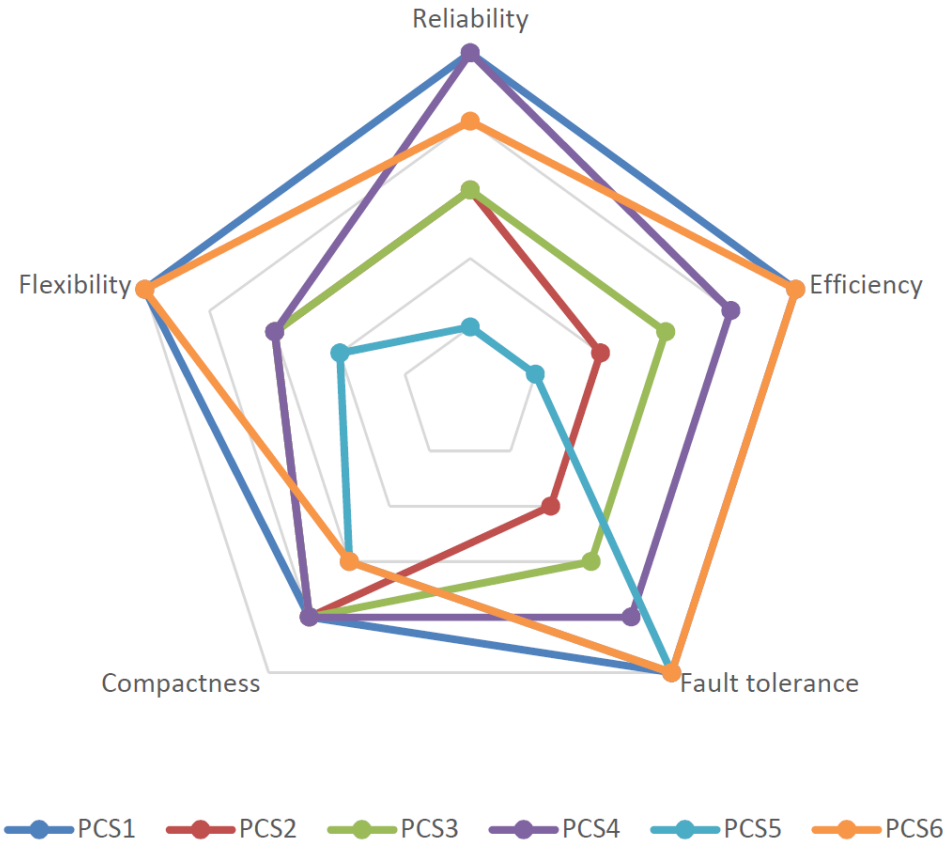

Figure 6: Comparison synthesis among PCSs.

4. Assessment on the interaction with network devices

Power electronics technologies start to be used in LV network system to manage the grid as result of the renewable energy systems. This new asset is a valuable solution in smart grids, but it is very important to determine the way how they are connected to the secondary substations (SS) in terms, for instance: i) The integration in the electrical environment; ii) fulfillment with electrical and telecommunication current regulations; iii) to ensure that such new devices are not seeing as an intrusive equipment for the electrical sector, mainly for the electrical workers, maintaining the same level of security and availability; iv) the avoidance of undesired counteractions with existing electrical protections. These aspects, among others, are discussed in section 4.1.

In turn, section 4.2 contains the cyber security considerations for the RESOLVD Energy Router (ER). Due to the preliminary state of the project, some aspects could not be considered in full details, as they have to be defined in alignment with specifications to be made in later work packages. Also, due to the universality of some of the topics in this section, there will be a considerable amount of overlap with other specification documents, especially with deliverable D1.4 Information Security requirements.

4.1. Practical aspects for the grid integration of the Energy Router

The following aspects are considered as important for the design of the Energy Router, addressing their integration into LV grids and interaction with other network devices:

- **The proximity of the ER to a secondary substation.** The ER could be installed in the proximity to a secondary substation. According with the segmentations of the LV network, the problem arises when the ER tries to start up and this part of the network or secondary substation operating at very low loading index. Under such circumstances, the short circuit impedance of the grid seeing by the ER could be so low, mainly determined by the leakage inductance of the LV side of the transformer at the SS. This may compromise the voltage stability of the network while the ER is starting up. This problem should be taken into account while designing the control algorithms of the ER.
- **Electromagnetic compatibility (EMC) compatibility with other network devices.** All electric devices or installations influence each other when interconnected or close to each other by radiation or conducted communication signals. In a SS, this problem it is known as a noise and it could interference power line communications (PLC) systems, automation systems, electronics relays, and etcetera. The purpose of EMC is to keep all those side effects under reasonable control. EMC designates all the existing and future techniques and technologies for reducing disturbance and enhancing immunity. The Electromagnetic Compatibility Directive 2014/30/EU ensures that electrical and electronic equipment does not generate, or is not affected by, electromagnetic disturbance. The EMC Directive limits electromagnetic emissions from equipment in order to ensure that, when used as intended, such equipment does not disturb radio and telecommunication, as well as other equipment. The Directive also governs the immunity of such equipment to interference and seeks to ensure that this equipment is not disturbed by radio emissions, when used as intended.
- **Protection issues while building up islands.** Distributed generation could potentially feed unplanned system islands. Such unplanned islanded mode implies a significant safety risk for the equipment and workers. So that, it needs to be quickly detected and eliminated. One way to be able of detecting islands is by sensitive under- and over-voltage and frequency functions, sometimes aided by active island destabilization techniques. Both the passive voltage and frequency trip point and active destabilization measures to counter islanding, however, can also adversely impact to system dynamic performance. As distributed generation penetration grows, attention will need to be paid

to avoid unplanned islands, and the impact of measures used to detect and eliminate islands on system performance when no islanding occurs. For this, the ER need to be operated in terms to ensure the operational under safety criteria. However there are other features to take care of, for instance the technology needs to ensure that the selectivity about overcurrent protections are operated taking into account that power electronics systems have not short circuit capability, just overcurrent. This is especially important to coordinate when the electrical system is operated in coupled grid or it is working in islanded mode. Also, there is another question to be considered when it will be necessary to return from island mode to grid connected, which is the synchronism features such as difference of the frequency, the phase and the modules of the voltage among the islanded part of the grid and the main grid.

- **Proper protections operation of other network devices while in islanded mode.** The neutral point of the LV network from the SS involved in the pilot area must be always available to ensure that the residual-current protection device (or as known, ground fault circuit interrupter) must operate when the electrical system detected a residual current and also, to ensure that the star system is not unbalanced in voltage thus avoiding overvoltage. In Spain, the LV electrical distribution system is three-phase, although there are others that can be used. There are two types of subscribers in LV, three-phase and single phase ones, but the distribution system is only three-phase. Single phase subscribers receive electricity with a voltage of 230 V and three phase subscribers at 400 V. The three phase distribution system has a voltage across phases of 400 V and, of 400 / √ 3) = 230 V between phase and neutral. Thus, single phase subscribers are supplied through the phase and neutral conductors. A three-phase system has grounded the neutral conductor, because it does not have a potential difference with the ground, it has a "0 V voltage". The masses are also grounded, it is what is called ground protective and its sole purpose is to safeguard people. Hence the Neutral grounded and metallic points grounded, as well. The neutral serves to achieve the 230 V of single-phase subscribers, among other things. It will be necessary to place it on the ground often to guarantee this power of 0 V and that the single-phase system maintains the 230 V between phase and neutral.
- **Electrical resonances with other network components.** Electrical resonances exist in all circuits including inductances and capacitances, possibly resistances as well. This is a phenomenon that occurs in electrical power systems of all voltage levels. The necessary and sufficient conditions are the framework of scenarios where resonance develops. The capacitors in electrical networks are linear elements. Nevertheless, the inductances may be both type: linear and nonlinear (with ferromagnetic core) and all kind of converters use non lineal devices as a load seen from the electrical system. While is true that only one resonance steady state may appear in a linear circuit with certain value of capacitance and inductance, it is significant that resonance frequency may be different with the frequency of energy source. In this case, nonlinear inductance is not taken part in resonance circuit directly, but it generates harmonic components. The nonlinear resonance may be excited in circuits with linear capacitors and nonlinear inductances. Resonances can cause big overvoltage in power systems at any voltage level, so they should be taken into account while designing the passive inductive and capacitive filters of the ER.
- **Synchronization with the grid after the isolated mode: "Seamless transfer"**. This situation is a feasible operation of micro-grids. The RESOLVD network could be addressed as several potential islanded areas or as several micro-grids built up by distributed generators and consumptions. Such islanded micro-grids may have to be connected to the main grid again and this is a challenging task because the voltage, phase and frequency levels should match with those for the grid at the connection point. Although frequencies may match perfectly, it may happen that the interconnector switch cannot be turned on due to phase difference and the likely voltage module differences.

The installation of separate equipment for the phase difference control would give us the best solution. Also, the phasor measurement unit (PMU) will be crucial to monitoring these variables to ensure the optimal electrical operation in this situation.

- **Earth connection of battery packs**. Regulations are flexible on this matter. The design of the ER in this matter has to fulfill the requirements of the current regulations of LV equipment and grids. Work in [56] explains the way how to do the grounding that it is established primarily in order to limit the tension that, with respect to earth, may present at a given moment the metallic masses, ensure the performance of the protections and eliminate or reduce the risk of a breakdown in electrical equipment used. When other technical instructions prescribe the mandatory ground of some element or part of the installation, said grounding is shall be governed by the content of this instruction. The voltage for the DC interconnection cable isolation must be at the maximum 0,6-1 kV for voltage level less than 1 kV. When the battery operates at a voltage level more than 60 V, it will require the installation of a failure detector. The section of the ground conductors have to satisfy the need according the ITC BT-18, must be of 25 mm2 (copper) and also, the section shall not be less than the minimum required for drivers' protection. The risks of electrification and even electrocution for each one of the different schemes of ground connection, as defined by the International Electro-technical Commission in the IEC 60364 standard.
- **Environmental aspects.** Environmental aspects such as the humidity and temperature must be taken in care in terms to give the optimal operation requirements of the battery. The electrical environment certainly is heavy due at the variability of the climatic items. In the SS, it is possible to achieve more than 60ºC inside in summer season or -15 ºC in winter season. That's means that the battery and power electronics must be designed with effective cool and heating system to ensure the optimal operation avoiding internal damages. For instance, the optimum operating temperature for lithium-ion batteries is between -10 and 30 degrees Celsius. Low temperatures do not affect the useful life, but the actual available power that the battery can deliver, and cause the autonomy to be reduced. Regarding the batteries of lead-acid, these are designed to operate at 20-25ºC. Low temperatures affect the performance of batteries and reduce their lifespan.
- **Easy installation of the ER in the low voltage grid**. New smart grid technologies in the DSO sector should be adopted ensuring that these are to be welcomed by the technicians of the electrical sector. This is an important issue to take into account and it implies that new technology should not be intrusive in regard of the traditional operation procedures of the distribution networks. Also, the new development should be easy installed.
- **Secure operation in case of failure of communications with the rest of the network.** In this sense, it is important to differentiate which devices needs to stop after a telecommunication problem occurs and which need to keep working. For instance, the ER could still improve the power quality level at its connection point in case of failure of communications but it is an open question whether it might have to take decisions on other operational actions of the grid under such communications failure. The Intelligent Local Energy System (ILEM) that the ER equips would have the responsibility to manage the distributed devices nearby.

4.2. Cybersecurity assessment

4.2.1. Architecture overview

From an ICT perspective, the ER consists basically of an industrial PC running a Linux system, connected via serial Modbus (EIA-485)/CAN to a power electronics system. The latter is out of scope of this assessment, as it belongs to the power plane and does not have any ICT interfaces, except for the one connecting it to the industrial PC. Via the PC, the ER has two further main communication interfaces (see Figure 7).

- A Modbus (TCP/IP) interface to the gateway device to be developed in WP3;
- A TCP/IP interface to the cloud platform to be developed in WP4.

Due to the early stage of the project, the systems in WP3 (the *Wide Area Monitoring Systems – WAMS* – Gateway and attached devices) and WP4 (cloud platform) have not been defined yet. This leaves the interface specification recommendations given in this section in a preliminary state, which is subject to change depending on the demand of later work within the project.

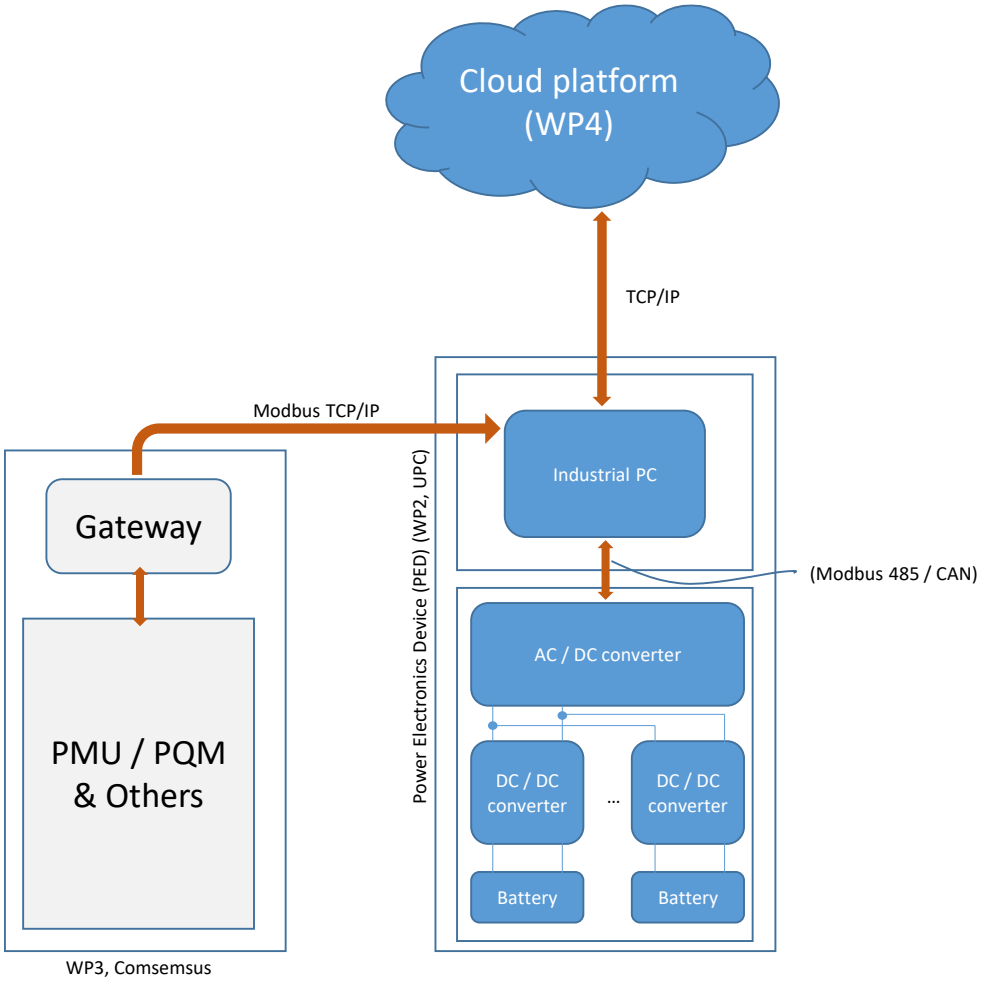

Figure 7: Device and communication architecture of the Energy Router.

4.2.1. Threat model

In order to structurally identify potential cyber security threats to the ER, we use *threat modeling* [78]. Using this technique, we model the involved entities and the data flow between them and introduce *trust boundaries*. The resulting model can be analyzed for structural weaknesses. To do so, we used a threat modeling tool (the *Microsoft Threat Modeling Tool 2016* [67]), that is capable of providing a diagram of the model and automatically identifying a number of threat categories using the STRIDE methodology (see Section 4.2.1.1).

4.2.1.1. Attacker model

An adversary targeting the ER may have many potential goals (the list is non-exhaustive):

- Extract information to draw conclusions on power consumptions, user behavior and billing information;
- Extract information to achieve credentials to administrative accounts;
- Manipulate values to achieve altered billing;
- Take over the device to alter power flows;
- Issue commands that stop the device from functioning;
- Manipulate values to evoke illegal conditions that damage the device;

Technique to achieve this can be categorized into the following (according to the STRIDE methodology [67]):

- Spoofing of user identity.
- Tampering.
- Repudiation.
- Information disclosure (privacy breach or data leak).
- Denial of service (DoS).
- Elevation of privilege.

These techniques are to be considered to be main assets of an adversary capable to attack the ER in the following threat model.

4.2.1.2. Assumptions and limitations

We assume that an adversary does not have physical access to the device (see Section 4.2.2) and that the device is not used for other purposes than the operation of the ER, meaning that no unrelated processes or interfaces that are not immediately or indirectly (support operating system functions) necessary for the ER.

We further assume, that the ER is located in a restricted area inside the operating DSO's network, meaning that it is not subject to any threats from the DSO's internal network. A means to achieve this is to place it in an extra virtual LAN (VLAN) and appropriate Network Access List/Firewalling that allows only the three types of network access defined in Section 4.2.3.1.

As a result, threats to the communication flows between the industrial PC hosting the ILEM and the power plane with the BMS are not considered in the threat model.

The ER communication flows to and from the WAMS Gateway and the cloud platform are modelled with IPsec and HTTPS connections, respectively, instead of using protocols without security services, as this is regarded state-of-the-art practice. This is, however, reflected in the corresponding sections later on. Furthermore, as the WAMS Gateway is considered to be an external service from the ER's perspective, security measures in the WAMS Gateway operator's sphere of influence but affecting the relation to the ER are considered to be subject to a Service Level Agreement (SLA) to induce the former to maintain appropriate cyber security measures.

Analogously, the relation to the cloud platform is assumed to be an external service, making it untrusted and letting the relation to be governed by a SLA (see Section 4.2.6). Therefore problems solely in the influence of the cloud platform are considered to be compliance issues. It is further assumed that the cloud service is a *push service*, meaning that data processing has to be induced by ER and the platform is not actively *pulling* data from the ER.

Further, for simplification, the system internals of the industrial PC are not modelled. Instead, the ILEM is treated as an atomic entity.

4.2.1.3. Data flow

For the threat model, four bidirectional information flows are considered (see Figure 8):

- The administrative traffic between the device and its human operator;
- between the ILEM part (i.e. the industrial PC) and the Cloud Platform;
- between the ILEM and the WAMS gateway;
- between the ILEM and the BMS (via Modbus).

The latter flow, however, is out of scope (for the rationale see Section 4.2.1). On basis of these flows, cyber threats to the ER were identified (see Section 4.2.1.4) and, subsequently, mitigation strategies were defined.

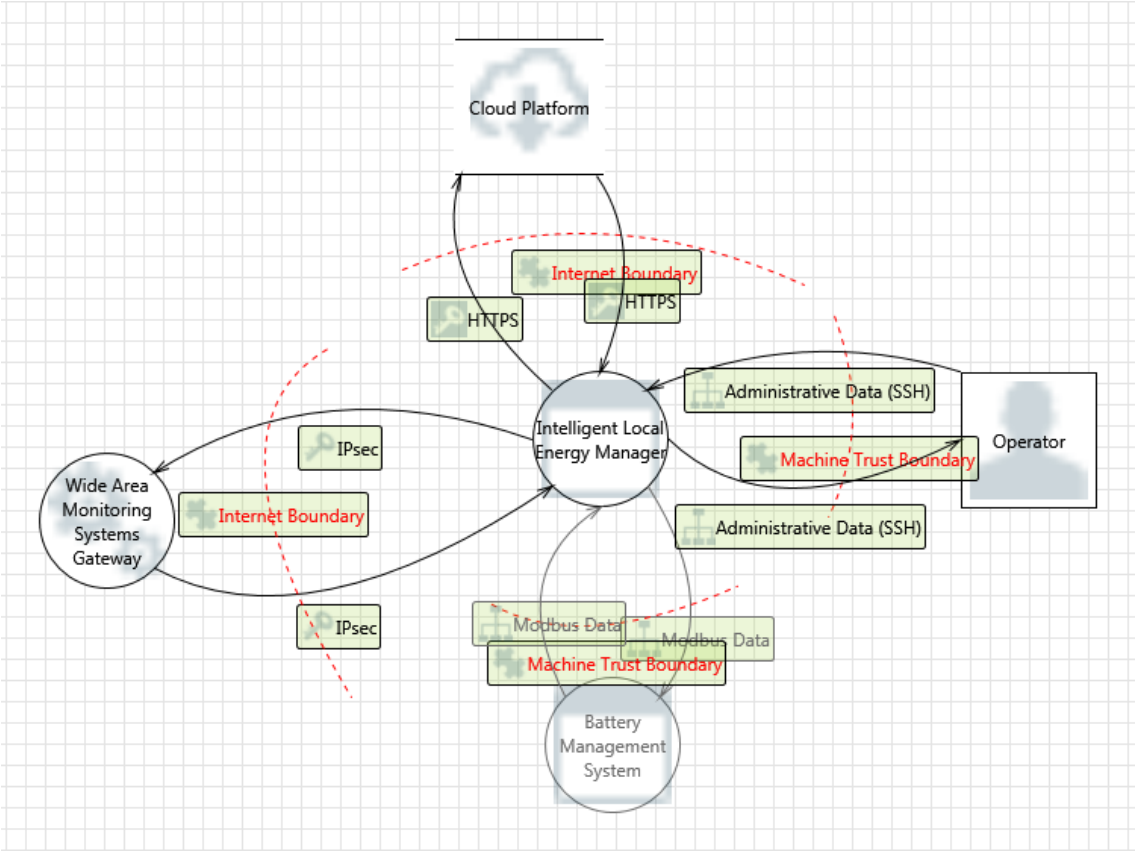

Figure 8: Diagram of the modelled ER information flows

4.2.1.4. Identified threats

The following Table 8 contains the automatically identified threats by the threat modeling tool according to the information flows described in Section 4.2.1.3. This information is complemented by a mitigation strategy and the section number where the appropriate measure is addressed.

No.	Description	Components	Category	Main Mitigation	Section
1	Data Flow Generic Data Flow Is Potentially Interrupted	ILEM, Operator	DoS	Network redundancy	4.2.5

No.	Description	Components	Category	Main Mitigation	Section
2	External Entity Operator Potentially Denies Receiving Data	ILEM, Operator	Repudiation	Logging	4.2.4.1
3	Spoofing of the Operator External Destination Entity	ILEM, Operator	Spoofing	Authentication	4.2.4, 4.2.3.1
4	Elevation by Changing the Execution Flow in Intelligent Local Energy Manager	ILEM, Operator	Privilege Elevation	Firewall, IDS, application whitelisting	4.2.3
5	Intelligent Local Energy Manager May be Subject to Elevation of Privilege Using Remote Code Execution	ILEM, Operator	Privilege Elevation	Identity management and appropriate permissions	4.2.3, 4.2.4
6	Data Flow Generic Data Flow Is Potentially Interrupted	ILEM, Operator	DoS	Network redundancy	4.2.5
7	Potential Process Crash or Stop for Intelligent Local Energy Manager	ILEM, Operator	DoS	Monitoring and reaction	4.2.4.1
8	Potential Data Repudiation by Intelligent Local Energy Manager	ILEM, Operator	Repudiation	Logging[1]	4.2.4.1
9	Elevation Using Impersonation	ILEM, Operator	Privilege Elevation	Authentication	4.2.5
10	Elevation by Changing the Execution Flow in Intelligent Local Energy Manager	ILEM, Cloud	Privilege Elevation	Firewall, IDS, application whitelisting	4.2.3
11	Intelligent Local Energy Manager May be Subject to Elevation of Privilege Using Remote Code Execution	ILEM, Cloud	Privilege Elevation	Identity management and appropriate permissions	4.2.3, 4.2.4
12	Data Store Inaccessible	ILEM, Cloud	DoS	N/A[2]	4.2.1.2
13	Data Flow HTTPS Is Potentially Interrupted	ILEM, Cloud	DoS	Network redundancy	4.2.5
14	Potential Process Crash or Stop for Intelligent Local Energy Manager	ILEM, Cloud	DoS	Monitoring and reaction	4.2.4.1
15	Weak Access Control for a Resource	ILEM, Cloud	Information Disclosure	Authorization, storage security	4.2.4, 4.2.6

[1] While the ILEM will not actively repudiate the reception of data, traceability might still be an asset in case of a cyber incident.

[2] The data store would in this case be the ILEM. Since the latter is meant to push data to the cloud platform, the availability of the same is assumed at the same time the upload is requested.

No.	Description	Components	Category	Main Mitigation	Section
16	Potential Data Repudiation by Intelligent Local Energy Manager	ILEM, Cloud	Repudiation	Logging[1]	4.2.4.1
17	Risks from Logging	ILEM, Cloud	Tampering	Source authentication[3]	4.2.5
18	Spoofing of Source Data Store Cloud Platform	ILEM, Cloud	Spoofing	Authentication	4.2.5
19	Spoofing of Destination Data Store Cloud Platform	ILEM, Cloud	Spoofing	Authentication	4.2.5
20	Risks from Logging	ILEM, Cloud	Tampering	Source authentication[3]	4.2.5
21	Lower Trusted Subject Updates Logs	ILEM, Cloud	Repudiation	Role-based identity management	4.2.4
22	Data Logs from an Unknown Source	ILEM, Cloud	Repudiation	Log access permissions	4.2.4.1
23	Insufficient Auditing	ILEM, Cloud	Repudiation	Authentication	4.2.5
24	Potential Weak Protections for Audit Data	ILEM, Cloud	Repudiation	Tamper-proof Backups	4.2.4.1
25	Potential Excessive Resource Consumption for Intelligent Local Energy Manager or Cloud Platform	ILEM, Cloud	DoS	Rate Limiting	4.2.3
26	The Cloud Platform Data Store Could Be Corrupted	ILEM, Cloud	Tampering	Integrity checking, Backups	4.2.5, 4.2.6
27	Data Store Denies Cloud Platform Potentially Writing Data	ILEM, Cloud	Repudiation	Logging	4.2.4.1
28	Data Flow HTTPS Is Potentially Interrupted	ILEM, Cloud	DoS	Network redundancy	4.2.5
29	Data Store Inaccessible	ILEM, Cloud	DoS	SLAs	4.2.6
30	Elevation by Changing the Execution Flow in Intelligent Local Energy Manager	ILEM, WAMSGW	Privilege Elevation	Firewall, IDS, application whitelisting	4.2.3
31	Intelligent Local Energy Manager May be Subject to Elevation of Privilege Using Remote Code Execution	ILEM, WAMSGW	Privilege Elevation	Identity man-agement and appropriate	4.2.3, 4.2.4

[3] This threat refers to log data by small data loggers. This is not an issue with the Cloud Platform or the ILEM, as these do not meet this profile. However, it is addressed in terms of not accepting data from untrusted sources.

No.	Description	Components	Category	Main Mitigation	Section
				permissions	
32	Data Flow IPsec Is Potentially Interrupted	ILEM, WAMSGW	DoS	Network redundancy	4.2.5
33	Potential Process Crash or Stop for Intelligent Local Energy Manager	ILEM, WAMSGW	DoS	Monitoring and reaction	4.2.4.1
34	Potential Data Repudiation by Intelligent Local Energy Manager	ILEM, WAMSGW	Repudiation	Logging[1]	4.2.4.1
35	Elevation Using Impersonation	ILEM, WAMSGW	Privilege Elevation	Authentication	4.2.5
36	Elevation Using Impersonation	ILEM, WAMSGW	Privilege Elevation	Authentication	4.2.5
37	Elevation by Changing the Execution Flow in Wide Area Monitoring Systems Gateway	ILEM, WAMSGW	Privilege Elevation	SLAs	4.2.3
38	Wide Area Monitoring Systems Gateway May be Subject to Elevation of Privilege Using Remote Code Execution	ILEM, WAMSGW	Privilege Elevation	SLAs	4.2.3
39	Data Flow IPsec Is Potentially Interrupted	ILEM, WAMSGW	DoS	Network redundancy	4.2.5
40	Potential Process Crash or Stop for Wide Area Monitoring Systems Gateway	ILEM, WAMSGW	DoS	SLAs	4.2.3
41	Potential Data Repudiation by Wide Area Monitoring Systems Gateway	ILEM, WAMSGW	Repudiation	Logging	4.2.4.1

Table 8: Identified Threats through Threat Modeling

4.2.2. Physical device security

Physical access to a device potentially allows for a variety attacks at very low cost. For instance, the Stuxnet worm, which has become a notorious example for a successful attack against industrial facilities, may have its origin in an infection via a USB flash drive [36]. Furthermore, physical access-based attacks may even nullify the protections given by a Trusted Platform Module [96]. Therefore direct plugin-in access to system hardware and hardware interfaces must be prohibited by organizational (strict permission checking) and technical (i.e. tamper-proof door locks) measures. More concrete requirements will be part of Deliverable *D1.4 Information Security Requirements*.

4.2.3. Device security

For all software running on the ER (specifically the Linux operating system and the operational services for the ER itself), the *principle of least privilege* (or *whitelisting*) should be applied.

This includes, but is not limited to the following:

- Deactivating unneeded interfaces (network – see Section 4.2.3.1 – and hardware);

- Deactivating unneeded system accounts and changing the default credentials for needed ones;
- Minimal possible privileges and file permissions for user and system accounts in general;
- Anti-DoS and brute force measures such as rate limiting and account locking after a number of failed attemts;
- The use of secure passwords;
- Using basic network defense concepts such as firewalling also on device level;
- *Application Whitelisting* per host-based IPS, file system permissions and/or other concepts such as *AppArmor* or utilizing the *SELinux* kernel extensions;
- Using a specialized, hardened kernel;
- Using redundancies and fault tolerance systems to ensure the system's availability.

Following the concept of *defense in depth*, access control (segregation, authentication, authorization) should not only occur at pivotal network points (*perimeter*), but also on every device, especially on critical systems, as otherwise overcoming perimeter security by introducing a compromised device may corrupt the security of all system devices. Therefore, the ER should not only rely on network-based defenses, but also have such systems running at the host itself. This includes basic defenses as host-based or personal firewalls (e.g. *iptables*) and intrusion detection systems (e.g. *Tripwire*, *AIDE* or *Ossec*). As well as basic protection on file system level, using permissions and *jails* and more advanced concepts as application level permissions using *SELinux* and/or *AppArmor*.

Furthermore, all user and system accounts should have secure passwords (see Section 4.2.4). If there are special service accounts necessary, they should only be used for that service alone and also no network login should be allowed using these accounts (e.g. using a *null shell*).

To further reduce the attack surface, a hardened Kernel could be used, which is a custom-compiled Kernel that contains only the functionality that is directly necessary for operating the service (including the necessary supporting security functions). Using such is a suggestion for ideal conditions, as it requires some effort on keeping the Kernel up to date, but on the other hand can greatly reduce the vulnerability and, thus, the attack surface of the overall system.

In order to sustain the availability of the ER, appropriate measures to provide continued power supply (e.g. redundant power supplies, *Uninterruptible Power Supplies – UPS*) should be provided along with redundant network connection (see Section 4.2.5) and monitoring to identify service and device failures (see Section 4.2.4.1).

4.2.3.1. Network access to the Energy Router

As with any access restrictions, the *principle of least privilege* (or *whitelisting*) should be applied, allowing only the following means of access:

- Necessary administrative interfaces;
- a well-defined interface to gateway;
- a well-defined interface to the cloud service.

Therefore, remote configuration interfaces must not be available on public interfaces, ideally only from internal networks. If off-site remote administration is imperative, the interface should only be available over a secured VPN interface. For remote administration, only secure, encrypted and authenticated protocols, such as Secure Shell (SSH) should be used. If this is not possible, they should be secured by tunneling the respective protocol, for instance by binding the interface to *localhost* only and *forwarding* the respective secure interface to the localhost. When using such secured interfaces, two factor authentication (2FA) and cryptographic methods, such as *public key authentication* are favorable. As with all other

interfaces (but in this case with special importance, due to the broader capabilities and, thus, threat potential), as less administrative interfaces as possible should be in place. If an insecure web interface is mandatory for the functioning of the ER, this interface should be secured by using a *reverse proxy* (e.g. *nginx*) that runs on a secured (*TLS-protected* – see Section 4.2.5) port that redirects after successful authentication to the insecure port on *localhost* only. For both cases described above, if the respective insecure administrative service cannot be bound to a localhost-only interface, a firewall has to block non-local machine access to the same.

As the internal Modbus interface does not run on TCP/IP (see Section 4.2.5.3), it is not considered a network access. The Gateway interface should consist of an IPsec interface to the RESOLVD gateway device (for further specification, see Section 4.2.5.1), while the interface to the cloud service should be not be an open port, but an ER-initiated TLS connection to the cloud service (see Section 4.2.5.2). To allow for administration of the server itself, we propose an SSH interface with user accounts as defined in Sections 4.2.3 and 4.2.4.

4.2.4. Identity management

Any accounts created should be role-based, restricting their permissions to the ones needed to fulfill their very purpose. One role, for instance, should be the one of the ILEM itself, transmitting to and receiving data from the cloud platform. When this account is the only one authorized to do so, this should prevent information disclosure from through the cloud, provided that the data stored in the cloud is accordingly protected (see Section 4.2.6).

Proposed Roles for human actors are:

- Auditor (read logs);
- Admin (full system);
- Operator (ER-related files and processes)
- System service (liberal system access);
- Network service (very restricted system access).

Actual user accounts to fill in these roles, however, should only be created when needed.

In any case, all of the created accounts must be protected by strong, non-default, state-of-the-art passwords (e.g. following the latest version of the recommendations of the NIST [24]) and be protected against brute force attacks (by rate limiting and/or lockout procedures). Alternatively they may be protected by public key cryptography (i.e. certificate-based authentication, see also [54] for a more sophisticated concept). Remote accounts should also contain a second factor protection (realized via a 2-factor authentication in a VPN system).

Also, the authentication, authorization and accounting (see Section 4.2.4.1) can be supported by an appropriate facility and protocol (e.g. Diameter or Kerberos).

4.2.4.1. Logging and monitoring

Any actions from system externals (i.e. human actors and remote machines) must be logged accordingly (accounting). This applies to data manipulation, but also to administrative tasks (e.g. stopping or starting a service). These logs should be also part of a backup (ideally using a system that does not allow a posteriori manipulation), to allow for traceability in case of an erroneously or deliberately precipitated system malfunction or failure. As the means to achieve this have to be adjusted to the nature of the data, it depends on the deployment of the ER, how tamper-proof the logs have to be (simple logging might even be sufficient). Also, logs may only accessed by the respective service to belong to and by an operator with an according role (see Section 4.2.4).

To achieve proper functioning (availability of the service) of the ER, the device should be monitored by a corporate network management system. In case of one of the services to stop unexpectedly (i.e. a crash) or certain log conditions indicating a potential cyberattack, appropriate alerts should be generated and sent to responsible human actors, allowing pre-defined procedures to be invoked (e.g. a system reboot).To ease the log management, logs may be divided into alert classes. A suitable model for this is provided by the Syslog protocol [23]. This allows for a ruleset which person will be alerted under which conditions (ideally the network management system allows for an escalation chain to be defined), whereby the group of responsible people should correspond to their roles.

4.2.5.Communication line security

In order to protect communication line data flows (or data in transit), they should be protected in terms of providing confidentiality, integrity, authentication and replay protection. To protect recorded data from being deciphered a posteriori (after illegitimately acquiring secret keys), also *perfect forward secrecy* [25] is a desirable property of a secure connection. To provide this level of protection, cryptographic ciphers that are currently deemed secure should be used. Currently recommended cipher suites are the following [77]:

- DHE_RSA_WITH_AES_128_GCM_SHA256;
- ECDHE_RSA_WITH_AES_128_GCM_SHA256;
- DHE_RSA_WITH_AES_256_GCM_SHA384;
- ECDHE_RSA_WITH_AES_256_GCM_SHA384.

The authentication should be mutual and based on certificates, if feasible. In any case, the protection should be end-to-end (from device to device, not being terminated at some intermediate gateway). Further recommendations on cryptographic configurations, see Sections 4.2.5.1 and 4.2.5.2.

Network access should be provided in a redundant way in order to prevent connection loss by a introducing a single point of failure in form of a single communications line. This redundancy could be provided by locating the ER in a highly available data center.

4.2.5.1. Modbus TCP/IP external communication to the WAMS gateway

The Encapsulating Security Payload (ESP) of the Internet Protocol Security (IPsec) protocol stack [38] provides a means to provide security services for any IP protocol [39]. This makes IPsec with ESP, despite some disadvantages to the Transport Layer Security (TLS) protocol stack (see Section 4.2.5.2), to the best choice for securing a TCP-tunneled non-IP protocol such as Modbus TCP/IP. The recommendations about ciphers above are met by the standardized *Suite-B-GCM-128* and *Suite-B-GCM-256* [42]. As communication between two peers is used to be in *transport mode*, this mode should be used to establish an end-to-end connection (using mutual certificate-based authentication, as both peers should be known beforehand) to encapsulate the Modbus over TCP connection used by the ER and the WAMS gateway.

4.2.5.2. TCP/IP external communication to the cloud service

Other than the Modbus interface in Section 4.2.5.1, the cloud service can be secured using Transport Layer Security (TLS) [17], as, in principle, it has some advantages over other alternatives (such as IPsec) [3]:

- TLS is easier to integrate between different vendors;
- TLS needs less overhead;
- TLS allows quicker handshakes;

- TLS is easier to configure.

To provide safe configuration, the cipher suites in Section 4.2.5 have to be used. Furthermore the two peers (ER and cloud platform) should adhere to the following recommendations [53]:

- They Must negotiate the most recent version of TLS (currently 1.2[4]; exclusion of TLS 1.0 and 1.1, as well as Secure Sockets Layer - SSL);
- Must implement strict TLS and HTTP Strict Transport Security (HSTS) [31];
- Must disable TLS-level compression;
- DH keys of at least 2048 bits or ECDH keys of at least 192 bits must be used;
- No anonymous suite must be used;

Apart from the certificate-based authentication should be mutual, at least the cloud service must mandatorily authenticate itself this way.

4.2.5.3. Modbus 485 internal communication

As defined in Section 4.2.1.2, this communication is out of scope of these cyber security considerations.

4.2.6. Data storage security

In order to prevent potential problems from the cloud service provider's side, appropriate Service Level Agreements (SLAs) should be made. These should contain the availability of the cloud (for instance an availability of 99,999% or *five nines* would mean a downtime of approximately 15 minutes per year) and penalties for data breaches. Any data at rest in the cloud must be encrypted with a key in possession of the ER operator's organization. If feasible, that also applies to data on the move.

To protect the data at rest (including credentials and private keys), volumes should be encrypted, e.g. using DM-Crypt with LUKS (Linux Unified Key Setup). Analogous to data in transit, it is crucial to use state-of-the-art encryption. For LUKS this would be the newer standard cipher *aes-xts-plain64:sha256*, as the older *aes-cbc-essiv:sha256* contains vulnerabilities [75]. The access to the data should only be allowed in accordance with the defined roles (see Section 4.2.4). This especially applies to databases, which should support this role-based authentication concept (read/write/manipulate). Apart from that, any operation has to be logged (in the sense of Section 4.2.4.1).

To prevent data loss in case of a physical event, a large scale cyberattack or corrupted data, regular backups should be made. These backups should be checked for their functioning (i.e. restore drills) on a regular basis. The backups should be protected by the same (i.e. cryptographic) means as other stored data.

[4] The recommended cipher suites are, as combined authentication and encryption scheme not supported in prior versions, furthermore are all previous versions subject to known vulnerabilities.

5. Conclusions

This work addresses the architecture of the two main planes composing the Energy Router: i) a so-called power plane; and ii) a management plane. Thus, the present work serves as a starting point for the design of the ER in subsequent tasks. The power plane includes the components actually exchanging electrical power with the network the system is connected to, e.g. batteries and power electronics. In turn, the management plane is composed by those algorithms and related hardware managing the system. A kind of structure is adopted for the power electronics device with local storage, the Energy Router (ER) hereinafter, to be developed in RESOLVD project.

In regard of the power plane architecture, the present work developed a comparison among different PCSs for modular battery-based solutions. Six main PCSs, along with their corresponding variants were identified. Variants refer to the number of power conversion steps included in each of the modules composing the PCSs. A first classification of the different PCSs proposed in literature, patents and those actually developed by industry in projects serves to identify the parallel connection of different and independent power trains to a single point of common coupling with the network, as the most proliferated one, especially by industry in projects. This first classification also identified the structures based on MMCC as particularly explored by academia for research and development purposes. The large number of papers addressing such topologies supports this affirmation. After the above mentioned first classification, this work proposed a quantitative / qualitative comparison among the different PCSs, also including the different variants at module level. From this work, included in section 3.2, the authors conclude that PCS #1 (the parallel connection of different power trains to a single point of common coupling), is currently the most reliable, efficient, compact, flexible and with best performance in regard of fault tolerance, among eligible options. The quantitative comparison also identified PCS #6 (the parallel association of dc-dc conversion steps interfacing different battery packs to a single dc-link which in turn is connected to a three-phase inverter), as one promising option for modular battery-based solutions also. It offers excellent performance in regard of efficiency, flexibility and fault tolerance, with the potentiality of configuring a solution with less volume than PCS #1.

Further, the comparison identified MMCC-based PCSs (PCSs #2 through #4) as promising ones in the future, but with the need of overcoming the drawbacks of connecting different modules in cascade. Further even, the problems derived from connecting of modules in cascade are exacerbated in the PCS #5 (the cascaded association of dc-dc conversion steps interfacing different battery packs to a single dc-link which in turn is connected to a three-phase inverter), greatly affecting the reliability and efficiency of this topology.

As the principal outcome of the above exercise, the PCS #6 variant c) was determined as the most convenient one for the purposes of the present work. However PCS #1 is identified a slightly superior solution than PCS #6 currently, it is worth to investigate within RESOLVD project in PCS #6 as it has the potentiality to become a solution with similar performance of PCS #1 employing a less number of power converters. PCS #6 variant c) offers an excellent reliability, efficiency, compactness and behavior under grid faults. In addition, it offers excellent flexibility while integrating different batteries of different characteristics, thus addressing one of the main requirements for RESOLVD project.

Complementing the decision on the architecture of the power plane of the Energy Router, important aspects regarding the electrical integration of the device into networks have been identified. Such exercise results into a relevant list of issues that should be addressed at the time of actually designing the prototype of the ER in subsequent tasks of the project (e.g. the assessment of EMC noise, the easy installation of the device in grids and the operation of the ER under failures in communication systems, among others).

Finally, section 4.2 offers a first assessment on cybersecurity aspects to take into account at the time of designing the management plane of the ER. Work included a threat model, through which a list of 41 potential threats for the ER while interfacing with other network devices was

presented. After this first exercise, a first discussion on cybersecurity measures was presented. Several aspects were addressed, including the physical device security, the network access security, the logging and monitoring considerations, communication line security issues and data storage security.

Annexes

Annex 1: Reliability and efficiency block diagrams and mathematical expressions

Reliability block diagrams and corresponding mathematical expressions

Figure 9 to Figure 11 present the reliability block diagrams for PCS #1 through #5 (variant a)).

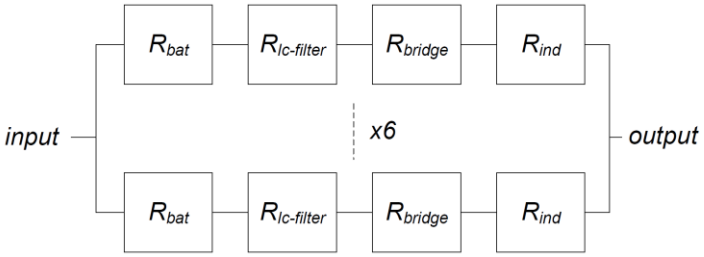

Figure 9: Reliability block diagram for PCS #1 and #4, variant a).

For PCS #1 and #4 variant (a), it reads:

$$R_{PCS1a} = R_{PCS4a} = 1 - \left(1 - R_{bat} \cdot R_{lc} \cdot R_{bridge} \cdot R_l\right)^6. \quad (29)$$

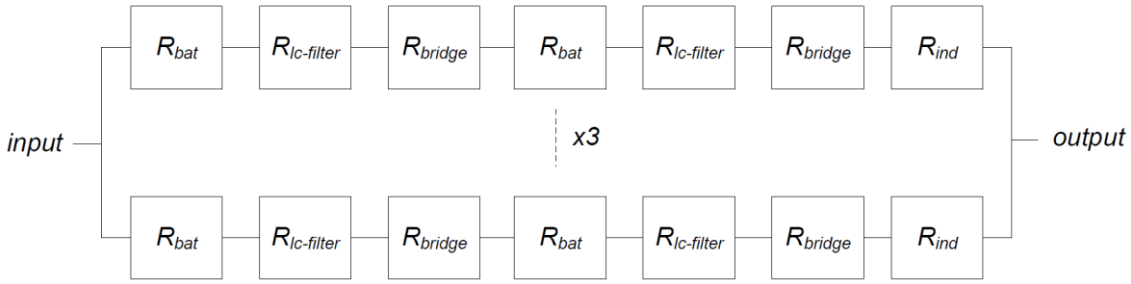

Figure 10: Reliability block diagram for PCS #2 and #3, variant a).

For PCS #2 and #3 variant (a), it reads:

$$R_{PCS2a} = R_{PCS3a} = 1 - \left(1 - \left(R_{bat} \cdot R_{lc} \cdot R_{bridge} \cdot R_l\right)^2\right)^3. \quad (30)$$

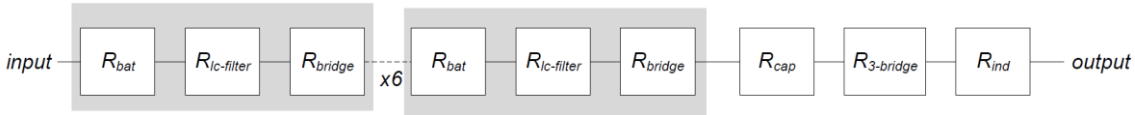

Figure 11: Reliability block diagram for PCS #5, variant a).

For PCS #5 variant (a), it reads:

$$R_{PCS5a} = R_{bat} \cdot R_{lc} \cdot R_{bridge} \cdot R_{cap} \cdot R_{3-bridge} \cdot R_l. \quad (31)$$

Efficiency block diagrams and corresponding mathematical expressions

Figure 12 present the efficiency block diagram for PCS #1 through #4 variant (a). The corresponding mathematical expression is depicted in the following:

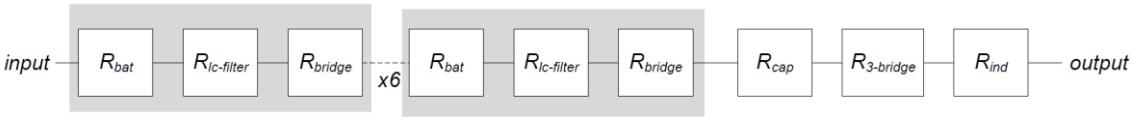

Figure 12: Efficiency block diagram for PCS #1 to PCS #4, variant (a).

$$\eta_{PCS1a} = \eta_{PCS2a} = \eta_{PCS3a} = \eta_{PCS4a} = \eta_{bat} \cdot \eta_{dc-ac}. \quad (32)$$

Annex 2: Simulation models

The selected PCS architecture for the ER is the type PCS #6c. Therefore, for subsequent exercises on detailed design and construction of a prototype, simulations models of 3-phase inverters and double active bridge dc-dc structures are needed. These are briefly presented in the following and will be utilized in Tasks 2.2 and 2.3 of RESOLVD project. The software adopted for simulation is Matlab Simulink.

3-phase H-bridge inverter model (non-averaged model)

In this model, the converter is represented by 4 MOSFETs configuring an H-bridge inverter. The functioning of such 1-phase inverter can be directly extrapolated to a 3-phase one and representing just 4 switches, computational effort while simulating is diminished. The dc-link is modelled as an ideal dc voltage source. The AC-grid is modelled as an ideal AC voltage source and an inductive filter is included interfacing the grid and the H-bridge. Since simulating the switching of IGBTs, the applicability of this model is two-fold: i) to evaluate the power losses of the converter; ii) to design the switching strategy for MOSFETs before implementing it on the prototype.

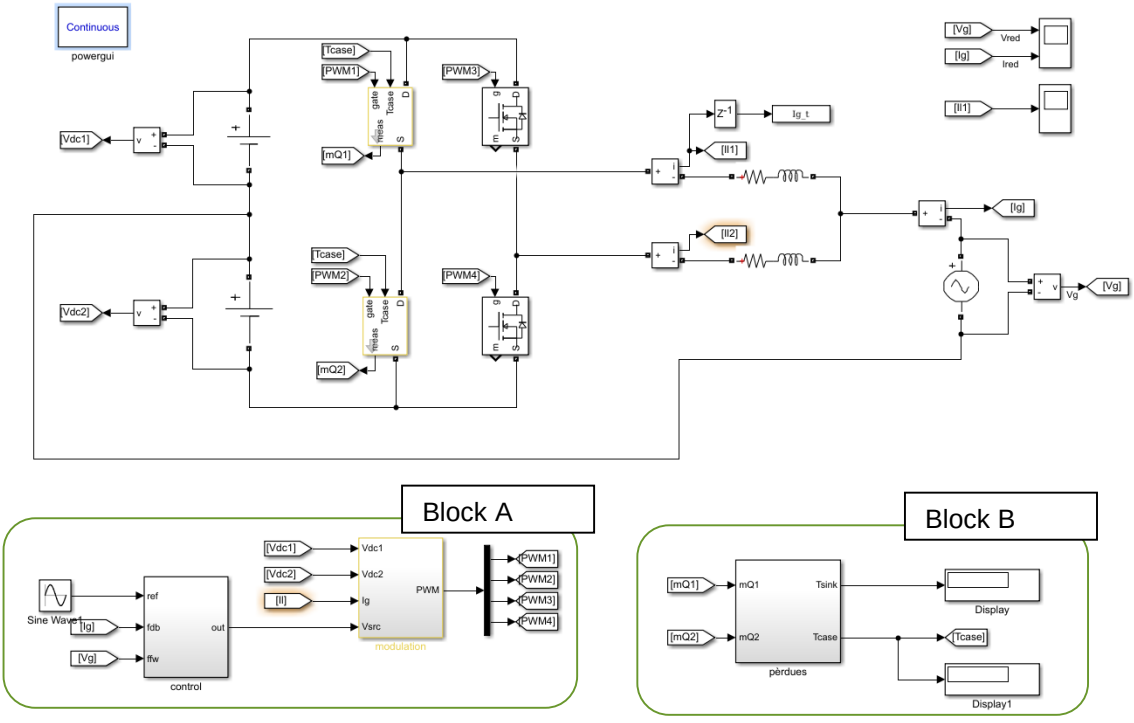

Figure 13: H-bridge inverter Matlab Simulink model.

For power losses calculation, the performance of transistors Q1 and Q2 (left branch) is temperature dependent and equations for losses calculation are embedded into block B, as depicted in Figure 13.

In turn, Block A includes the low level control algorithm managing the current and voltage at the AC terminals of the inverter. The control algorithm is based on a fractional proportional resonant current controller. Such controller offers an extra degree of freedom that enhances the response in frequency of the controller over conventional proportional resonant controllers. For more information on the tuning of such controller, the reader is referred to [28].

Finally, input parameters for the model are depicted in Table 9.

Parameter	Description	Parameter	Description
V_g	RMS grid voltage.	R	Resistance of the grid filter.
F_g	Grid frequency.	T_{air}	Ambient temperatura.
f_s	Switching frequency.	R_{th-sa}	MOSFET sink-air thermal resistance.
V_{DC}	Dc-link voltage.	R_{th-cs}	MOSFET case-sink thermal resistance.
L	Inductance for grid filter.	P	Rated power.

Table 9: Input parameters for the inverter's model.

Double active bridge dc-dc module (non-averaged model)

Similar to the H-bridge inverter, a detailed model for the dc-dc conversion modules in PCS #6c has been built. Figure 14 depicts the structure of the converter. As can be noted, the model details the MOSFETs building up the two H-bridges of the structure interfaced through a high frequency transformer.

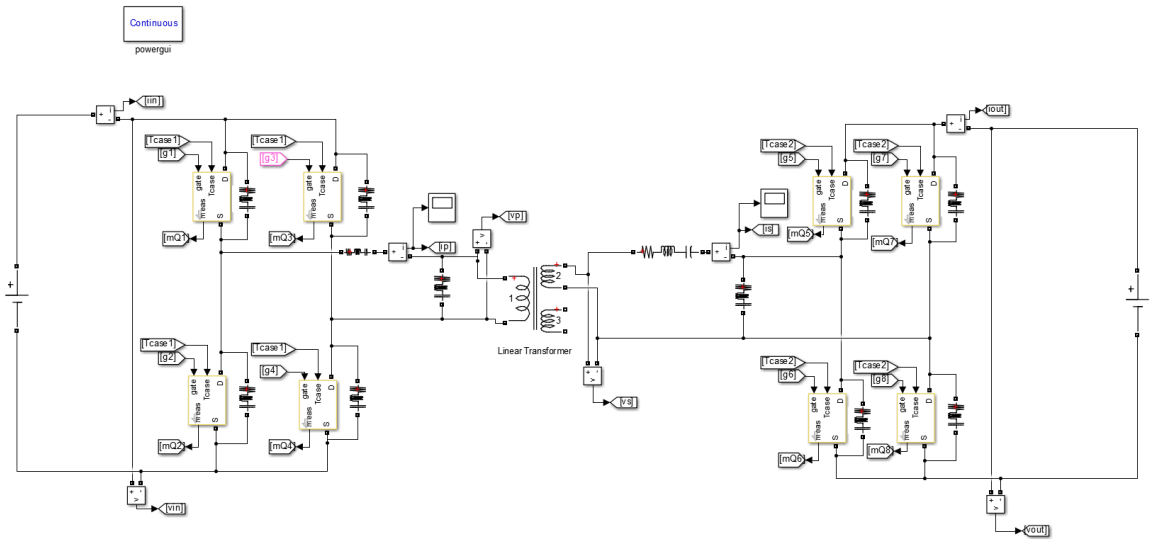

Figure 14: Double active bridge dc-dc converter.

The PWM switching is performed according to the duty cycles deduced from current control algorithms. The gate triggering signals for the MOSFETs of the H-bridges are the outputs of the following control blocks in Figure 15.

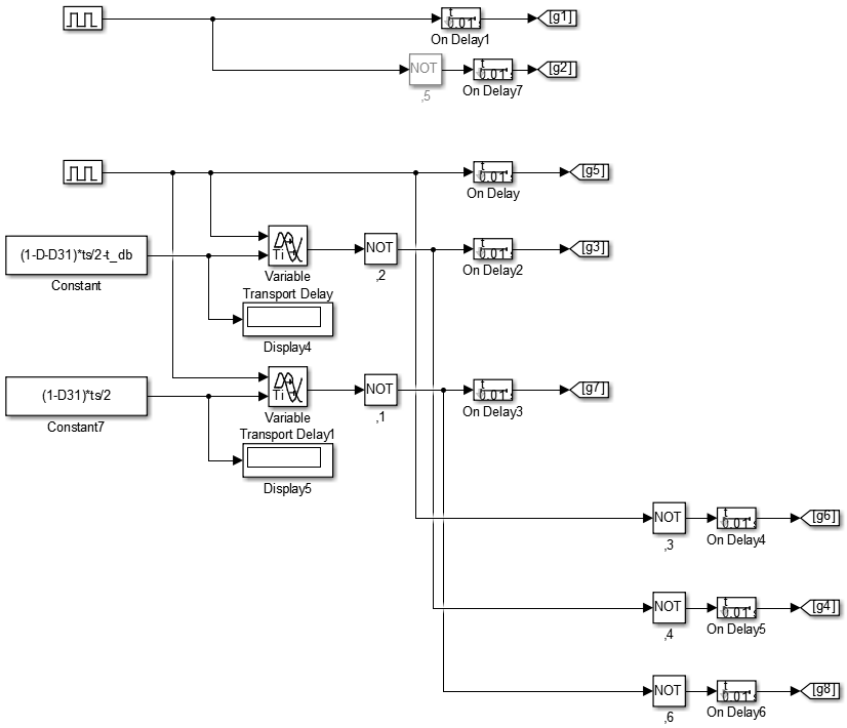

Figure 15: PWM control algorithm for the H-bridges of the double active bridge converter.

Finally, as noted in Figure 14, the model of the MOSFETs is temperature dependent and this feature enables the utilization of the model for power losses calculation. Such calculation is performed in the block detailed in Figure 16.

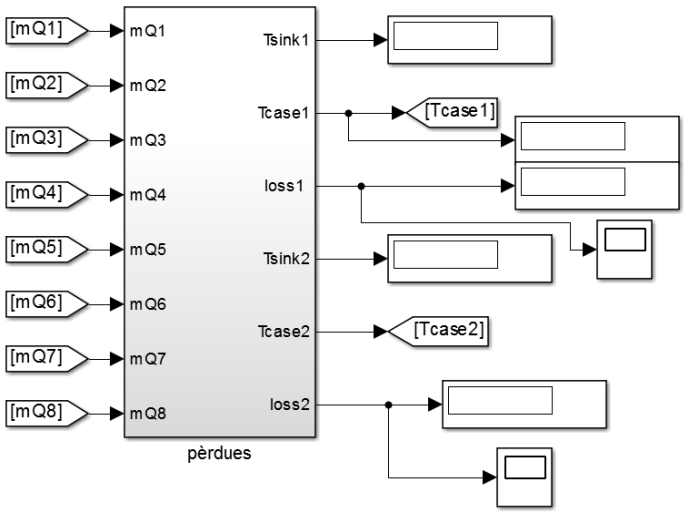

Figure 16: Block for power losses calculation for the double active bridge converter.

The input parameters for the model are listed in Table 10.

Variable	Description	Variable	Description
V_{in}	Input voltage.	V_{in-t}	Input voltage at transformer terminals.

Variable	Description	Variable	Description
V_{out}	Output voltage.	R_t	Transformation ratio.
P_n	Rated power.	r_{1-t}	Primary winding resistance.
f_s	Switching frequency.	l_{1-t}	Primary winding leakage inductance.
T_{db}	Delay time for MOSFETs gate signal.	r_{2-t}	Secondary winding resistance.
C_{MOSFET}	Stray capacitance of a MOSFET.	l_{2-t}	Secondary winding leakage inductance.
R_{MOSFET}	Internal resistance of a MOSFET.	l_{m-t}	Magnetizing inductance for the transformer.
T_{air}	Ambient temperature.	r_{m-t}	Core resistance for the transformer.
R_{th-sa}	MOSFET sink-air thermal resistance.	r_f	Resistance of LC filter at transformer terminals.
R_{th-cs}	MOSFET case-sink thermal resistance.	l_f	Inductance of LC filter at transformer terminals.

Table 10: Input parameters for the double active bridge model.

References

[1]. Adam, G.P., Anaya-Lara, O., Burt, G.M., Telford, D., Williams, B.W., McDonald, J.R. (2010) Modular multilevel inverter: pulse width modulation and capacitor balancing technique. IET Power Electronics, Vol. 3, No. 5, pp. 702-715

[2]. Akagi, H. (2011). Classification, terminology, and application of the modular multilevel cascade converter (MMCC). IEEE Transactions on Power Electronics, Vol. 26, No. 11, pp. 3119-3130

[3]. Alshamsi, A., & Saito, T. (2005). A technical comparison of IPSec and SSL. In 19th International Conference on Advanced Information Networking and Applications (Vol. 2, pp. 395-398). IEEE

[4]. D'Arco, S. Piegari, L., Tricoli, P. (2012) A modular converter with embedded battery cell balancing for electric vehicles. In: Electrical Systems for Aircraft, Railway and Ship Propulsion, pp. 1-6

[5]. Baruschka, L., Mertens, A. (2011). Comparison of cascaded H-bridge and modular multilevel converters for BESS application. In: Energy Conversion Congress and Exposition (ECCE), Phoenix, AZ, USA, pp. 909-916

[6]. Baker R.H., Bannister L.H. (1975) Electric power converter. US patent 3.867.643.

[7]. Bazargan D, Filizadeh S, Gole AM. (2014) Stability analysis of converter-connected battery energy storage systems in the grid. IEEE Transactions on Sustainable Energy, Vol. 5, No. 4, pp. 1204-1212

[8]. Bin, R., Yonghai, X., Qiaoqian, L. (2015) A control method for battery energy storage system based on MMC. In: IEEE 2nd International Future Energy Electronics Conference (IFEEC), Taipei, pp. 1-6

[9]. Bhowmik, S., Macris, E. (2010). Systems and methods for scalable configurations of intelligent energy storage packs. US patent number: US2010/0305770A1

[10]. Bragard, M., Soltau, N., Thomas, S., De Doncker, R.W. (2010). The balance of renewable sources and user demands in grids: power electronics for modular battery energy storage systems. IEEE Transactions on Power Electronics, Vol. 25, No. 12, pp. 3049-3056

[11]. Caponio, F., Abba, A., Baruzzi, P., Ripamonti, G., Geraci, A. (2011) Modular and bi-directional energy storage system compliant with accumulators of different chemistry. In: Electrical Power Quality and Utilisation (EPQU), Lisbon, Portugal, pp. 1-6

[12]. Cepin, M. (2011) Assessment of Power System Reliability. Springer-Verlag London Limited. DOI: 10.1007/978-0-85729-688-7-9

[13]. Chakraborty, S., Kramer, B., Kroposki, B. (2009) A review of power electronics interfaces for distributed energy systems towards achieving low-cost modular design. Renewable and Sustainable Energy Reviews, Vol. 13, pp. 2323-2335

[14]. Chang, F., Yang, Z., Wang, Y., Lin, F., Liu, S. (2015). Fault characteristics and control strategies of multiterminal high voltage direct current transmission based on modular multilevel converter. Mathematical Problems in Engineering, Article ID 502372, 11 pages, doi:10.1155/2015/502372

[15]. Chint Power Systems (2017) 30 kW storage inverter for North America. URL: https://www.chintpowersystems.com/. Accessed: 12.12.2017

[16]. Demetriades, G. (2014). Modular multilevel converter with cell-connected battery storages. US patent number: US8760122B2

[17]. Dierks, T., & Rescorla, E. (2008). The Transport Layer Security (TLS) Protocol Version 1.2 (RFC 5246). Internet Engineering Task Force. Internet Requests for Comments.

[18]. DOE global energy storage database. URL: https://www.energystorageexchange.org/. Accessed: 27.02.2018

[19]. Ferreira, A. (2017) Modular multilevel converters for power system applications. PhD Thesis. Universitat Politècnica de Catalunya. URL: https://upcommons.upc.edu/handle/2117/107948. Accessed: 25.02.2018

[20]. Fontana, E.C., Smith, P. (2010) System and method for combining the outputs of multiple, disparate types of power sources, US patent, publication number: US12831478

[21]. Gao, F., Zhang, L., Zhou, Q., Chen, M., Xu, T., Hu, S. (2014) State-of-charge balancing control strategy of battery energy storage system based on modular multilevel converter. In: IEEE Energy Conversion Congress and Exposition (ECCE), Pittsburgh, USA, pp. 2567-2574

[22]. General Electric. Dry type transformers for general purpose, aluminum, three-phase DOE 2016 efficiency. URL: http://www.geindustrial.com/buylog_pdf. Accessed: 12.12.2017

[23]. Gerhards, R. (2009). The Syslog Protocol (RFC 5464). Internet Engineering Task Force. Internet Requests for Comments.

[24]. Grassi, P., Fenton, J., Newton, E., Perlner, R., Regenscheid, A., Burr, W., Richer, J., Lefkovitz, N., Danker, J., Choong, Y.Y., Greene, K., Theofanos, M. (2017): Digital identity guidelines: authentication and lifecycle management (SP 800-63B). National Institute of Standards and Technology. NIST Special Publication.

[25]. Günther, C. G. (1989). An identity-based key-exchange protocol. In Workshop on the Theory and Application of of Cryptographic Techniques (pp. 29-37). Springer, Berlin, Heidelberg.

[26]. Hagiwara, M., Akagi, H. (2014). Experiment and simulation of a modular push–pull PWM converter for a battery energy storage system. IEEE Transactions on Industry Applications, Vol. 50, No. 2, pp. 1131-1140

[27]. Hart, D.W. (2011) Power Electronics. McGrau-Hill, pp. 477. ISBN-10: 0073380679

[28]. Heredero-Peris, D., Enric Sánchez-Sánchez, Chillon, C., Montesinos-Miracle, D., Galceran-Arellano, S. (2016) A novel fractional proportional-resonant current controller for voltage source converters. In: European Conference on Power Electronics and Applications, Karlsruhe, Germany, pp. 1-10

[29]. Hillers, A., Biela, J. (2013). Optimal design of the modular multilevel converter for an energy storage system based on split batteries. In: 15th European Conference on Power Electronics and Applications (EPE), Lille, pp. 1-11

[30]. Hillers, A., Biela, J. (2014). Fault-tolerant operation of the modular multilevel converter in an energy storage system based on split batteries. 16th European Conference on Power Electronics and Applications, Lappeenranta, pp. 1-8

[31]. Hodges, J., Jackson, C., & Barth, A. (2015). HTTP Strict Transport Security (HSTS) (RFC 6797). Internet Engineering Task Force. Internet Requests for Comments.

[32]. IEEE 90 – Institute of Electrical and Electronics Engineers, IEEE Standard Computer Dictionary: A Compilation of IEEE Standard Computer Glossaries. New York, NY, 1990

[33]. Jeanneret, R. (1995). Apparatus with discrete circuits for charging electrical accumulator with multiple group of cells. US patent number: US5412305.

[34]. Kanakasabai, V., Sen, B. (2013) Modular stacked dc architecture traction system and method of making same. US patent, application number: US20130134911A1

[35]. Kandasamy, K., Vilathgamuwa, M., Tseng, K.J. (2015). Inter-module state-of-charge balancing and fault-tolerant operation of cascaded H-bridge converter using multi-dimensional modulation for electric vehicle application. IET Power Electronics, Vol. 8, No. 10, pp. 1912-1919

[36]. Karnouskos, S. (2011). Stuxnet worm impact on industrial cyber-physical system security. In IECON 2011-37th Annual Conference on IEEE Industrial Electronics Society (pp. 4490-4494). IEEE.

[37]. Kawakami, N., Ota, S., Kon, H., et al. (2014). Development of a 500-kW modular multilevel cascade converter for battery energy storage systems. IEEE Transactions on Industry Applications, Vol. 50, No. 6, pp. 3902-3910

[38]. Kent, S. (2005). IP Encapsulating Security Payload (ESP) (RFC 4303). Internet Engineering Task Force. Internet Requests for Comments.

[39]. Kent, S., & Seo, K. (2005). Security Architecture for the Internet Protocol (RFC 4301). Internet Engineering Task Force. Internet Requests for Comments.

[40]. Kontos, E., Tsolaridis, G., Teodorescu, G. and Bauer, P. (2017). On DC Fault Dynamics of MMC-based HVDC Connections. IEEE Transactions on Power Delivery, Vol. PP, No. 99

[41]. Kubo, K., Nomura, T., Tokunaga, N., Miyazaki, H., Emori, A. Charge and discharge system for electric power storage equipment. US patent number: US6297616B1

[42]. Law, L., & Solinas, J. (2011). Suite B Cryptographic Suites for IPsec (RFC 4869). Internet Engineering Task Force. Internet Requests for Comments.

[43]. LI, B., He, J., Tian, J. et al. (2017). DC fault analysis for modular multilevel converter-based system. J. Mod. Power Syst. Clean Energy, Vol. 5, No. 2, pp. 275–282

[44]. Li, G., Liang, J., Ma, F., Ugalde-Loo, C.E., Liang, H. and Li, H. (2017). Analysis of single-phase-to-ground faults at the valve-side of HB-MMCs in bipolar HVDC systems. In: IEEE Energy Conversion Congress and Exposition (ECCE), Cincinnati, OH

[45]. Li, Y., Han, Y. (2016). A module-integrated distributed battery energy storage and management system. IEEE Transactions on Power Electronics. DOI: 10.1109/TPEL.2016.2517150

[46]. Lim, J.U., Lee, S.J., Kang, K.P. (2015). A modular power conversion system for zinc-bromine flow battery based energy storage system. In: IEEE 2nd International Future Energy Electronics Conference (IFEEC), Taipei, pp. 1-5

[47]. Liu, Z., Tan, C., Leng, F. (2015) A reliability-based design concept for lithium-ion battery pack in electric vehicles. Reliability Engineering and System Safety, Vol. 134, pp. 169-177

[48]. Magnetics Powder cores catalog (2011). URL: http://www.mag-inc.com/products/powder-cores. Accessed: 20.06.2016

[49]. Maharjan, L., Inoue, S., Akagi, H., Asakura, J. (2009). State-of-charge (SOC)-balancing control of a battery energy storage system based on a cascade PWM converter. IEEE Transactions on Power Electronics, Vol. 24, No. 6, pp. 1628-1636

[50]. Maharjan, L., Inoue, S., Akagi, H., Asakura, J. (2009). Fault-tolerant control for a battery energy storage system based on a cascade PWM converter. In: IEEE 6th International Power Electronics and Motion Control Conference, Wuhan, pp. 945-950

[51]. Maharjan, L., Yamagishi, T., Akagi, H. (2012). Active-power control of individual converter cells for a battery energy storage system based on a multilevel cascade PWM converter. IEEE Transactions on Power Electronics, Vol. 27, No. 3, pp. 1099-1107

[52]. Manjrekar, M.D., Steimer, P.K., Lipo, T.A. (2000) Hybrid multilevel power conversion system: a competitive solution for high-power applications. IEEE Transactions on Industrial Electronics, Vol. 49, No. 4, pp. 724-738

[53]. Marksteiner, S., & Vallant, H. (2017). Towards a secure smart grid storage communications gateway. In Smart City Symposium Prague 2017, Prague, Czech Republic (pp. 1-6). IEEE

[54]. Metke, A. R., & Ekl, R. L. (2010). Security technology for smart grid networks. IEEE Transactions on Smart Grid, 1(1), 99-107.

[55]. MIL-HDBK-217F(N2) Parts Count Prediction Calculator. URL: http://reliabilityanalyticstoolkit.appspot.com/mil_hdbk_217F_parts_count. Accessed: 25.02.2018

[56]. Ministerio de Ciencia y Tecnología, Spanish Government (2002). Real Decreto 842/2002, 2 de agosto, Reglamento electrotécnico para baja tensión. Reglamento electrotécnico para baja tensión e instrucciones técnicas complementarias (ITC) BT 01 a BT 51

[57]. Mitra, B., Chowdhury, B. (2017). Comparative analysis of hybrid DC breaker and assembly HVDC breaker. In: North American Power Symposium (NAPS), Morgantown, pp. 1-6

[58]. Mitsubishi power electronics website. URL: http://www.pwrx.com/. Accessed: 14.02.2018

[59]. Montesinos-Miracle, D., Massot-Campos, M., Bergas-Jané, J., et al. (2013). Design and control of a modular multilevel DC/DC converter for regenerative applications. IEEE Transactions on Power Electronics, Vol. 28, No. 8, pp. 3970-3979

[60]. Mukherjee, N., Strickland, D. (2012). Modular ESS with second life batteries operating in grid independent mode. In: 3rd IEEE International Symposium on Power Electronics for Distributed Generation Systems, Aalborg, pp. 653-660

[61]. Mukherjee, N., Strickland, D., Varnosfaderani, M.A. (2014). Adaptive control of hybrid battery energy storage systems under capacity fade. In: Power Electronics and Applications (EPE'14-ECCE Europe), 2014 16th European Conference on, Lappeenranta, Finland, pp. 1-10

[62]. Mukherjee, N., Strickland, D. (2015). Control of second-life hybrid battery energy storage system based on modular boost-multilevel buck converter. IEEE Transactions on Industrial Electronics, Vol. 62, No. 2, pp. 1034-1046

[63]. Mukherjee, N., Strickland, D. (2016). Control of cascaded DC–DC converter-based hybrid battery energy storage systems - Part I: stability issue. IEEE Transactions on Industrial Electronics, Vol. 63, No. 4, pp. 2340-2349

[64]. Mukherjee, N., Strickland, D. (2016). Control of cascaded DC–DC converter-based hybrid battery energy storage systems - Part II: Lyapunov approach. IEEE Transactions on Industrial Electronics, Vol. 63, No. 5, pp. 3050-3059

[65]. M5BAT (2015). M5BAT project website. URL: http://m5bat.de/de-de/Projekt. Accessed: 20.01.2016

[66]. Nice Grid EU project website. URL: http://www.nicegrid.fr/. Accessed: 21.02.2018

[67]. Potter, B. (2009). Microsoft SDL threat modelling tool. *Network Security*, *2009*(1), 15-18.

[68]. Prieto-Araujo E., Junyent-Ferré A., Collados-Rodríguez C., Clariana-Coleta G., Gomis-Bellmunt O. (2017) Control design of modular multilevel converters in normal and AC fault conditions for HVDC grids. Electric Power System Research, Vol. 152, pp. 424-437

[69]. Qahouq, J.A. (2014). Distributed battery power electronics architecture and control. US patent number: US20140125284A1

[70]. Quraan M., Yeo T., Tricoli P. (2016) Design and control of modular multilevel converters for battery electric vehicles. IEEE Transactions on Power Electronics, Vol. 31, No. 1, pp. 507-517

[71]. REO-USA, Inc. (2017) HPTA/603 transformer. URL: http://www.reo-usa.com/. Accessed: 12.12.2017

[72]. Rodriguez J, Lai J-S, Peng FZ. (2002) Multilevel inverters: a survey of topologies, controls, and applications. IEEE Transactions on Industrial Electronics, Vol. 49, No. 4, pp. 724-738

[73]. Rothgang, S., Baumhöfer, T., van Hoek, H., Lange, T., De Doncker, R.W., Uwe Sauer, D. (2015) Modular battery design for reliable, flexible and multi-technology energy storage systems. Applied Energy, Vol. 137, pp. 931-937

[74]. Sayed, K., Gabbar, H.A. (2016) Electric vehicle to power grid integration using three-phase three-level AC/DC converter and PI-fuzzy controller. Energies, Vol. 9, 532-548

[75]. Schmidt, J. (2013). Erfolgreicher Angriff auf Linux-Verschlüsselung. Heise, Hannover. Online: https://www.heise.de/security/artikel/Erfolgreicher-Angriff-auf-Linux-Verschluesselung-2072199.html (Retrieved 2018-03-12).

[76]. Sha D., Xu G., Xu Y. (2017) Utility direct interfaced charger/discharger employing unified voltage balance control for cascaded H-bridge units and decentralized control for CF-DAB modules. IEEE Transactions on Industrial Electronics, Vol. 64, No. 10, pp. 7831-7842

[77]. Sheffer, Y., Holz, R., & Saint-Andre, P. (2015). Recommendations for Secure Use of Transport Layer Security (TLS) and Datagram Transport Layer Security (DTLS) (RFC 7525). Internet Engineering Task Force. Internet Requests for Comments.

[78]. Shostack, A. (2014). Threat modeling: Designing for security. John Wiley & Sons.

[79]. Shousha, M., Prodic, A., Marten, V., Milios, J. (2017) Design and implementation of assisting converter based integrated battery management system for electromobility applications. IEEE Journal of Emerging and Selected Topics in Power Electronics, Article in press. DOI: 10.1109/JESTPE.2017.2736166

[80]. Siemens (2015). Siemens Siestorage product description. URL: http://w3.siemens.com/powerdistribution/global/en/mv/power-supply-solutions/siestorage/. Accessed: 20.01.2016

[81]. Soong, T., Lehn, P.W. (2014). Evaluation of emerging modular multilevel converters for BESS applications. IEEE Transactions on Power Delivery, Vol. 29, No. 5, pp. 2086-2094

[82]. Steinmetz Ch-P. (1984) On the law of hysteresis. Reprint, Proceedings of the IEEE, 72(2), pp. 196-221

[83]. Tan, N.M.L., Abe, T., Akagi, H. (2012) Design and performance of a bidirectional isolated DC–DC converter for a battery energy storage system. IEEE Transactions on Power Electronics, Vol. 27, No. 3, pp. 1237-1248

[84]. Tang, L., Ooi, B.T. (2007). Locating and isolating DC faults in multi-terminal DC systems. IEEE Transactions on Power Delivery, Vol. 22, No. 3, pp. 1877-1884

[85]. Thomas, S., Stieneker, M., De Doncker, R.W. (2011). Development of a modular high-power converter system for battery energy storage systems. In: 14th European Conference on Power Electronics and Applications, Birmingham, pp. 1-11

[86]. Tolbert, L.M., Peng, F.Z., Habetler, T.G. (1999). Multilevel converters for large electric drives. IEEE Transactions on Industry Applications, Vol. 35, No. 1, pp. 36-44

[87]. Tolbert, L.M., Peng, F.Z., Cunnyngham, T., Chiasson, J.N. (2002). Charge balance control schemes for cascade multilevel converter in hybrid electric vehicles. IEEE Transactions on Industrial Electronics, Vol. 49, No. 5, pp. 1058-1064

[88]. Trintis, I., Munk-Nielsen, S., Teodorescu, R. (2011) Cascaded H-bridge with bidirectional boost converters for energy storage. In: Power Electronics and Applications (EPE 2011), Birmingham, UK, pp. 1-9

[89]. Tsang, K.M., Chan, W.L. (2012). 27-Level DC–AC inverter with single energy source. Energy Conversion and Management, Vol. 53, pp. 99–107

[90]. Tsirinomeny M, Rufer A. (2015) Configurable modular multilevel converter (CMMC) for flexible EV. In: 17th European Conference on Power Electronics and Applications, Geneva, pp. 1-10

[91]. Uno M, Tanaka K. (2011) Influence of high-frequency charge-discharge cycling induced by cell voltage equalizers on the life performance of lithium-ion cells. IEEE Transactions on Vehicular Technology, 60(4), pp. 1505-1515

[92]. Vasiladiotis, M., Rufer, A. (2013) Balancing control actions for cascaded H-bridge converters with integrated battery energy storage. Power Electronics and Applications (EPE), 2013 15th European Conference on, Lille, pp. 1-10

[93]. Vasiladiotis, M., Rufer, A. (2015). A modular multiport power electronic transformer with integrated split battery energy storage for versatile ultrafast EV charging stations. IEEE Transactions on Industrial Electronics, Vol. 62, No. 5, pp. 3213-3222

[94]. Vasiladiotis, M., Rufer, A. (2015) Analysis and control of modular multilevel converters with integrated battery energy storage. IEEE Transactions on Power Electronics, Vol. 30, No. 1, pp. 163-175

[95]. Wall, S., McShane, D. (1997). A strategy for low-cost utility connection of battery energy storage systems. Journal of Power Sources, Vol. 67, pp. 193-200

[96]. Winter, J., & Dietrich, K. (2011). A Hijacker's Guide to the LPC Bus. In European Public Key Infrastructure Workshop (pp. 176-193). Springer, Berlin, Heidelberg.

[97]. Xie, B., Liu, Y., Ji, Y., Wang, J. (2018) Two-stage battery energy storage system (BESS) in AC microgrids with balanced state-of-charge and guaranteed small-signal stability. Energies, Vol. 11, pp. 322-336

[98]. Yang, J., Fletcher, J.E. and O'Reilly, J. (2012). Short-circuit and ground fault analyses and location in VSC-based DC network cables. IEEE Transactions on Industrial Electronics, Vol. 59, No. 10, pp. 3827-3837

[99]. Yutaka-Ota, J.Y., Sato, T., Akagi, H. (2016) Enhancement of performance, availability, and flexibility of a battery energy storage system based on a modular multilevel cascaded converter (MMCC-SSBC). IEEE Transactions on Power Electronics, Vol. 31, No. 4, pp. 2791-2799

[100]. Young, C.M., Chu, N.Y., Chen, L.R., Hsiao, Y.C., Li, C.Z. (2013). A single-phase multilevel inverter with battery balancing. IEEE Transactions on Industrial Electronics, Vol. 60, No. 5, pp. 1972-1978

[101]. Zhao, B., Song, Q., Liu, W., Sun, Y. (2014) Overview of dual-active-bridge isolated bidirectional DC–DC converter for high-frequency-link power-conversion system. IEEE Transactions on Power Electronics, Vol. 29, No. 8, pp. 4091-4106

[102]. Zhang, X.N., Zhao, C.Y. and Pang, H. (2013). A control and protection scheme of multi-terminal DC transmission system based on MMC for DC line fault, automation of electric power system, Vol. 37, No. 15, pp. 140-145

[103]. Zhang, Y., Ge, Q., Zhang, R., Du, Y. (2012) The control of arm currents and the parameters for modular multilevel converters. In: 15th Int. Conf. Elect. Mach. Syst., Sapporo, Japan, pp. 1-6

[104]. Zhang, Z., Cai, Y.-Y., Zhang, Y., Gu, D.J., Liu, Y.F. (2016) A distributed architecture based on microbank modules with self-reconfiguration control to improve the energy efficiency in the battery energy storage system. IEEE Transactions on Power Electronics, Vol. 31, No. 1, pp. 304-317